UPPSALA
UNIVERSITET

Digital Comprehensive Summaries of Uppsala Dissertations from the Faculty of Science and Technology 1855

Prospective Applications of Microwaves in Medicine

Microwave Sensors for Orthopedic Monitoring and Burn Depth Assessment

SYAIFUL REDZWAN MOHD SHAH

ACTA
UNIVERSITATIS
UPSALIENSIS
UPPSALA
2019

ISSN 1651-6214
ISBN 978-91-513-0753-4
urn:nbn:se:uu:diva-393105

Dissertation presented at Uppsala University to be publicly examined in Häggsalen, Ångströmlaboratoriet, Lägerhyddsvägen 1, Uppsala, Tuesday, 5 November 2019 at 09:15 for the degree of Doctor of Philosophy. The examination will be conducted in English. Faculty examiner: Professor Luca Roselli (High Frequency Electronics (HFE)-LAB, Department of Engineering, University of Perugia, Perugia, Italy).

Abstract
Redzwan Mohd Shah, S. 2019. Prospective Applications of Microwaves in Medicine. Microwave Sensors for Orthopedic Monitoring and Burn Depth Assessment. *Digital Comprehensive Summaries of Uppsala Dissertations from the Faculty of Science and Technology* 1855. 96 pp. Uppsala: Acta Universitatis Upsaliensis. ISBN 978-91-513-0753-4.

In recent years, the use of microwave techniques for medical diagnostics has experienced impressive developments. It has demonstrated excellent competencies in various modalities such as using non-ionizing electromagnetic waves, providing non-invasive diagnoses, and having the ability to penetrate human tissues within the GHz range. However, due to anatomical, physiological, and biological variations in the human body, certain obstacles are present. Moreover, there are accuracy problems such as the absence of numerical models and experimental data, difficulty in conducting tests due to safety issues with human subjects, and also practical restrictions in clinical implementation. With the presence of these issues, a better understanding of the microwave technique is essential to further improve its medical application and to introduce alternative diagnostic methods that can detect and monitor various medical conditions in real time.

The first part of this thesis focuses on measurement systems for the microwave technique in terms of sensor design and development, numerical analysis, permittivity measurement, and phantom fabrication. The aim is to investigate the feasibility of flexible systems with different fields of application including a microwave sensor system for measuring the healing progression of bone defects present in lower extremity trauma, bone regeneration in craniotomy for craniosynostosis treatments, and dielectric variation for burn injuries. The microwave sensor which utilizes the contrast in dielectric constant between various tissues was used as the primary sensor for the proposed application. This involved detailed optimization of the sensor for greater sensitivity. The experimental work carried out in the lab environment showed that the microwave sensor was able to detect the contrast in dielectric properties so that it can give an indication of the healing status for actual clinical scenarios.

The second part of the thesis is making a significant step towards its practical implementation by establishing a system that can detect and monitor the rate of healing progression with fast data acquisition speed of microseconds, and developing an efficient user interface to convert raw microwave data into legible clinical information in terms of bone healing and burn injuries. As an extension to this thesis, clinical studies were conducted and ethical approval for conducting tests on human subjects was obtained for the development of a microwave medical system. The results showed a clear difference in healing progressions due to high detection capability in terms of dielectric properties of different human tissues. All of these contributions enable a portable system to complement existing medical applications with the aim of providing more advanced healthcare systems.

Keywords: Microwave sensors, split ring resonator, biomedical application, orthopedics, lower extremity injuries, craniosynostosis, burn assessment, clinical measurements, tissue dielectric properties, phantom

Syaiful Redzwan Mohd Shah, Department of Engineering Sciences, Solid State Electronics, Box 534, Uppsala University, SE-75121 Uppsala, Sweden.

ISSN 1651-6214
ISBN 978-91-513-0753-4
urn:nbn:se:uu:diva-393105 (http://urn.kb.se/resolve?urn=urn:nbn:se:uu:diva-393105)

Genggam bara api, biar sampai jadi arang!

To my family, to my friends

List of Papers

This thesis is based on the following papers, which are referred to in the text by their Roman numerals.

I **Mohd Shah, S. R.**, Velander, J., Mathur, P., Perez, M. D., Asan, N. B., Kurup, D. G., Blokhuis, T. J., and Augustine, R. Split-ring resonator sensor penetration depth assessment using in vivo microwave reflectivity and ultrasound measurements for lower extremity trauma rehabilitation. *Sensors,* 2018, 18(2):636.

II Raaben, M., **Mohd Shah, S. R.**, Augustine, R., and Blokhuis, T. J. COMplex Fracture Orthopedic Rehabilitation (COMFORT) - Real-time visual biofeedback on weight bearing versus standard training methods in the treatment of proximal femur fractures in the elderly: study protocol for a multicenter randomized controlled trial. *Trials,* 2018, 19(1):220.

III **Mohd Shah, S. R.***, Velander, J.*, Perez, M. D., Joseph, L., Mattsson, V., Asan, N. B., Huss, F., and Augustine, R. Improved sensor for non-invasive assessment of burn injury depth using microwave reflectometry. *Proceeding of the 13th European Conference on Antennas and Propagation*, Krakow, Poland, 31 Mar.–5 Apr., EUCAP 2019.

IV **Mohd Shah, S. R.**, Mattsson, V., Velander, J., Perez, M. D., De Varies, E., Asan, N. B., Nowinski, D., Kurup, D. G., and Augustine, R. Microwave-sensor-based clinical measurement for monitoring post-craniotomy bone development in pediatric craniosynostosis patients. Submitted to *Sensors.*

V **Mohd Shah, S. R.**, Asan, N. B., Velander, J., Ebrahimizadeh, J., Perez, M. D., Mattsson, V., Blokhuis, T. J., and Augustine, R. Analysis of thickness variation in biological tissues using microwave sensors for health monitoring applications. Submitted to *IEEE Access*.

*The authors contributed equally to the work.

Author’s Contributions

I. Work conceptualization. Planning and performing all the experimental work. Took part in discussion and made major contribution in writing the manuscript.

II. Analyzing and interpreting the patient data regarding weight bearing after proximal femur fractures in the elderly. Took part in discussion and made minor contribution in writing the manuscript.

III. Work conceptualization. Planning and performing part of the experimental works including fabrications and ex-vivo measurement. Took part in discussion and made significant contribution in writing the manuscript.

IV. Work conceptualization. Planning and performing all the experimental works, including BDA system development, clinical measurement and the corresponding data fitting. Took part in discussion and major contribution in writing the manuscript.

V. Work conceptualization. Planning and performing all the experimental work, including fabrications, phantom measurement. Took part in discussion and major contribution in writing the manuscript.

Other contributions

I **Mohd Shah, S. R.**, Asan, N. B., Velander, J., Lee, D., Perez, M. D., Raaben, M., Blokhuis, T. J., and Augustine, R. Frequency domain analysis of hip fracture using microwave Split Ring Resonator sensor on phantom model. *2016 IEEE Asia-Pacific Conference on Applied Electromagnetics (APACE)*, Langkawi, Dec 2016, 244–247.

II Perez, M. D., **Mohd Shah, S. R.**, Velander, J., Raaben, M., Asan, N. B., Blokhuis, T. J., and Augustine, R. Microwave sensors for new approach in monitoring hip fracture healing. *2017 11th European Conference on Antennas and Propagation (EUCAP)*, Paris, Mar. 2017, 1838–1842.

III Asan, N. B., Penichet, C.P., **Mohd Shah, S. R**., Noreland, D., Hassan, E., Rydberg, A., Blokhuis, T. J., Voigt, T., and Augustine, R. Data packet transmission through fat tissue for wireless intra-body networks. *IEEE J. Electromag. RF Microw. Med. Biol.,* 2017, 1(2), 43–51.

IV **Mohd Shah, S. R.**, Velander, J., Mathur, P., Perez, M. D., Asan, N. B., Kurup, D., Blokhuis, T. J., and Augustine, R. Penetration depth evaluation of split ring resonator sensor using in-vivo microwave reflectivity and ultrasound measurements. *12th European Conference on Antennas and Propagation (EuCAP 2018)*, London, Apr. 2018, 1–5.

V Velander, J., **Mohd Shah, S. R.**, Perez, M. D., Asan, N. B., Blokhuis, T. J., and Augustine, R. Multi-functional phantom model to validate microwave sensors for health monitoring applications. *12th European Conference on Antennas and Propagation (EuCAP 2018)*, London, Apr. 2018, 1–5.

VI Asan, N. B., Hassan, E., Velander, J., **Mohd Shah, S. R**., Noreland, D., Blokhuis, T. J., Wadbro, E., Berggren, M., Voigt, T., and Augustine, R. Characterization of the fat channel for intra-body communication at r-band frequencies. *Sensors,* 2018, 18(9):2752.

VII Augustine, R.., Kurup, D. G., **Mohd Shah, S. R**., Mathur, P., Raman, S., Lee, D., and Kim, K. Microwave reflectivity analysis of bone mineral density using ultra wide band antenna. *Microw. Opt. Technol. Lett.*, 59: 21–26.

Contents

Abbreviations

Abbreviation	Description
2-D	2 Dimension
3-D	3 Dimension
ATE	Artificial tissue emulating
BDA	Bone Density Analyzer
BDAS	Bone Density Analysis System
CCL	Copper clad laminates
COMFORT	Complex Fracture Orthopedic Rehabilitation
CSF	Cerebrospinal fluid
CST	Computer simulation technology
CT	Computed tomography
DEXA	Dual-energy X-ray absorptiometry
DI	Deionized
E-field	Electric field
EM	Electromagnetic
EMS	Elderly mobility scale
FAC	Functional ambulation categories
FLIR	Forward-looking infrared
GHz	Gigahertz
H2020	Horizon 2020
H-field	Magnetic field
HF	High-frequency
ISM	Industrial, scientific and medical
LDPI	Laser Doppler perfusion imaging
MHz	Megahertz
MMG	Microwaves in Medical Engineering Group
MMUC	Maastricht Medical University Center
MMSE	Mini-Mental State Examination
MRI	Magnetic resonance imaging
MSI	Microwave sensing and imaging
MUT	Material under test
MWT	Microwave tomography
PDMS	Polydimethylsiloxane
QCT	Quantitative computed tomography
RF	Radio frequency
RCT	Randomized controlled trial

SMA	Subminiature version A
SPIRIT	Standard Protocol Items: Recommendations for Interventional Trials
SRR	Split ring resonator
TBI	Traumatic brain injury
TBSA	Total body surface area
UV	Ultraviolet
VAS	Visual analogue scale
VNA	Vector network analyzer

1 Introduction

A growing interest in medical technology can be attributed to society's increasing awareness of the importance of staying healthy in order to improve the quality of life. This leads to the demand for quality healthcare which has strained current healthcare systems, resulting in a lack of workforce and insufficient medical facilities. Therefore, the development of extensive and affordable consumer-based devices to meet healthcare demands is of high importance. One emerging technology is a method of applying radio frequency (RF) using microwaves (frequency range of 300 MHz to 300 GHz) for diagnostic and therapeutic purposes in medical applications.

In the years 1938 to 1939, Hollman from Germany suggested the use of microwaves for therapeutic purposes, which predicted that deep tissue heating could be produced by the electromagnetic (EM) waves without excessive skin heating.[1] A similar work was proposed by Hemingway and Stenstrom from the United States in 1939, which reviewed the high-frequency waves (short wavelength). They focused on a method of applying heat using microwaves for therapeutic purposes in medicine.[2] However, due to a lack of microwave sources and strict limitations on clinical trials, the use of microwave frequency was limited to only 100 MHz. In the early 1980s, the feasibility of using microwaves for diagnostic and therapeutic purposes increased rapidly.[3–7] There is an increasing interest in the research and development of medical applications based on microwave techniques, thanks to the fast development of semiconductor technology and numerous signal processing methods.

Microwave medical applications can be divided into three fundamental groups depending on how the microwaves are used:

1. Microwaves can be used for the treatment of patients (e.g. hyperthermia and diathermy). It is used for thermal or non-thermal effects.
2. Microwaves can be used to diagnose diseases with the aid of permittivity or attenuation measurements and can be used to generate tomographic images.
3. Microwaves can be used as a data telemetry tool.

1.1 State-of-the-art microwave medical technologies

In the present time, standard imaging technologies such as ultrasound, magnetic resonance imaging (MRI), computed tomography (CT), and X-ray are being widely used in the medical field for cancer diagnosis, bone imaging, tumor detection, musculoskeletal disorders, appendicitis, infectious diseases, and trauma. These methods provide clinical information concerning image contrasts between different tissues, provide good resolution, and some of the methods depend on ionizing radiation. For instance, MRI scanning provides good resolution, but is a costly procedure and has a fairly long examination time.

CT and X-ray are methods with intrinsic hazards as both methods use ionizing radiation and, hence, increase the risk of cancer. In addition, patients will have to tolerate mammography-related pain and discomfort during examinations. The ultrasound technique does not involve ionizing radiation and is preferred for diagnostic imaging in specific indications. However, due to its strong reflections that cause acoustic shadows, it cannot penetrate air and bones.[8–9] Moreover, it is operator-dependent and is not sensitive enough for specific areas, i.e. the detection of retroperitoneal hematoma. In comparison to the problems and risks associated with these technologies, the microwave method for medical applications has the potential to enhance both diagnostic capability and accuracy and also allows for earlier diagnosis. Microwave technology is based on non-ionizing EM waves, which makes it less harmful for patients compared to mammography and CT scan. In addition, the microwave method offers a non-invasive diagnosis in medicine which can reduce pain, improve the efficiency of treatments, and shorten the recovery time for patients.

The primary microwave applications in the medical field currently include data telemetry, medical diagnosis, and medical treatment, as shown in Figure 1.1. The following sections briefly present these three applications.

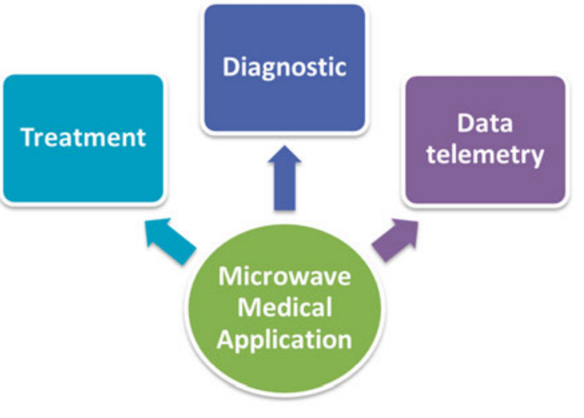

Figure 1.1 The main prospective applications of microwaves in medicine.

1.1.1 Microwave medical treatment

Microwave medical treatment is a method based on thermal effect. Heat is produced using microwave radiation to increase the local temperature in order to eliminate abnormal tissues (malignant). This method is more precise and effective compared to other modalities such as chemical toxins (chemotherapy), ionizing radiation (X-ray), and surgical treatment.[10–11] Other related microwave medical treatments include microwave thermotherapy, hyperthermia, and microwave ablation.[12–15]

In the context of this thesis, microwave medical treatment will not be covered. Instead, this thesis focuses on the usage of microwaves for diagnosis and monitoring which can be considered as a telemedicine system.

1.1.2 Microwave medical diagnosis

The incorporation of non-ionizing EM waves in the range of microwave frequency for sensing and imaging in medical diagnosis is becoming more prominent as it is affordable and poses a lower health risk compared to the aforementioned imaging technologies. The concept of microwave medical diagnosis is by observing the signal scattering produced by dielectric difference. In this process, there is a contrast of dielectric properties between healthy and malignant tissues.[16–18]. In terms of imaging, an image is created in a 2-D or 3-D form. This demonstrates a difference between dielectric properties (relative permittivity and conductivity) of various tissues or a difference between imaging and medical diagnosis. It is also possible to form an image based on differences in permittivity and position of an intense scattering that is a general indication of a tumor inside the body.

The spectrum of microwave sensing and imaging (MSI) of medical diagnosis covers several applications such as heartbeat detection, blood flow and pressure, fluid or water accumulation, brain stroke, and traumatic brain injury (TBI).[19–23] In microwave medical diagnosis, researchers have been using two main approaches intensively which are microwave tomography (MWT) and radio detection and ranging (radar) imaging.

In MWT and radar-based imaging, several wideband antennas (with high-range resolution) are placed surrounding the body. The antennas are formed based on a fixed array, matched with homogenous matching medium and use imaging algorithms to generate an image of the body.[24–26] MWT is based on reconstructing the distribution of complex permittivity by solving the problems of reverse electromagnetic scattering.

1.1.3 Data telemetry

Data telemetry is referred to as wireless data transmission using EM waves between implanted medical devices and external devices. In recent years, implanted devices have gained considerable interest among healthcare providers due to the rise in quality of life and a growing market for healthcare products.

Potential applications of data telemetry include deep brain stimulation, diabetic glucose surveillance, and cochlear implants.[27–29] For the application of cochlear implants, an external antenna attached behind the ear to the receiver in the cochlea (cochlear implant) can directly transmit audio signals. In diabetic glucose surveillance, glucose concentration is registered by an implanted biosensor and transferred to external devices by an implantable antenna. Other potential applications for data telemetry include blood pressure, heartbeat rate, intracranial pressure, and body temperature.

Up to the present time, there are no other available techniques better suited for data telemetry between implanted devices and external devices than microwaves. Galvanic and capacitive coupling are two approaches that could be used for the data telemetry concept. The reason for this is that microwaves allow wireless communication through human tissues which considerably increases the quality of life instead of using conventional implanted wire-based systems.

1.2 Telemedicine: challenges and opportunities

Telemedicine can be defined as the usage of telecommunication to transmit health information to healthcare clinics from a distance. It has been practiced for many decades in several medical applications to monitor health and diseases. In this method, patients' access to medical facilities can be significantly enhanced.

Today, thanks to the rapid development of technology, telemedicine can be employed with advanced images, audio, and video, interactive teleconferencing systems as well as live-streaming capabilities. For example, these technologies can expand the delivery of healthcare services to communities and individuals in suburban and rural areas. Furthermore, telemedicine can help to attract and maintain professional healthcare in rural areas by supporting ongoing training and collaborations with other healthcare professionals.

Figure 1.2 illustrates a vision of future telemedicine for a home health nursing service using microwaves. The system of medical diagnosis is used to monitor health issues such as cardiovascular diseases, burns, asthma, ENT (ear, nose, and throat), and stroke which need prompt diagnosis and treatment. In addition, telemedicine offers the opportunity to relay vital signs such as heart rate, blood pressure, diabetes (blood glucose), or respiration rate to a distant clinical professional and action can be initiated as needed. From this perspective, the combination of data telemetry and microwave medical diagnosis contributes effectively to an integrated healthcare system.

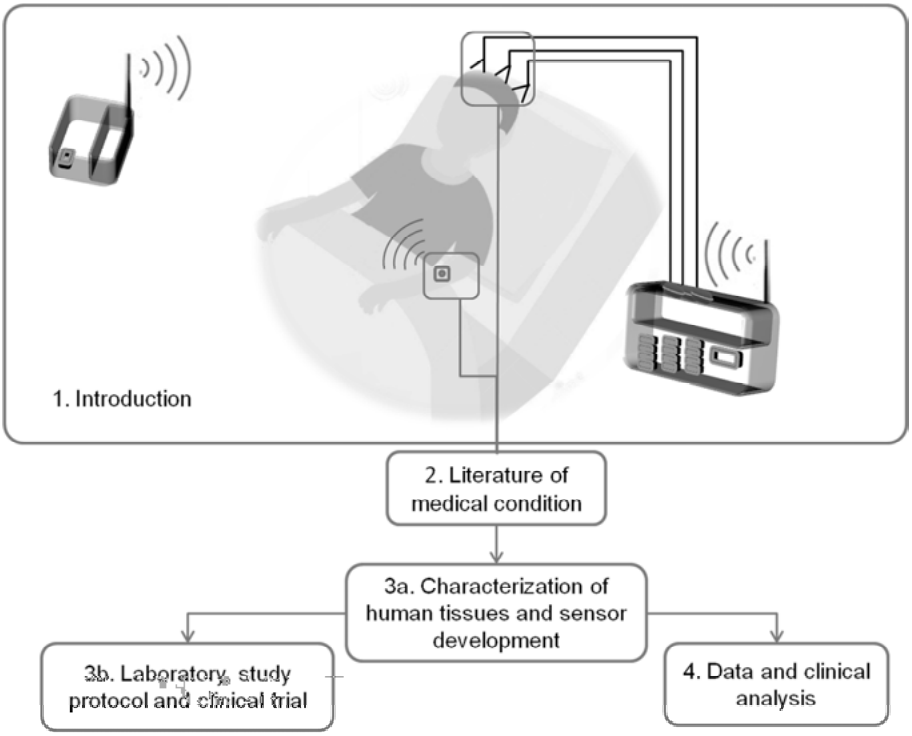

Figure 1.2 Illustration of telemedicine vision using microwaves for home health nursing service. The illustration also shows the aim as well as the scope of the work to comprehend these applications.

1.3 Outline of the thesis

This thesis presents the development of a medical diagnostic tool using the microwave technique that can be potentially used for the microwave healthcare system (see Figure 1.2). The focus is based on the concept of monitoring healing conditions on lower extremity fractures, craniosynostosis and burn injuries, with detailed explanations, which will be explained in Section 2. The dielectric properties (relative permittivity and conductivity) and sensor development have been studied to improve the understanding of the microwave techniques. The operational frequencies cover the range from 0.5 GHz to 10 GHz.

This work is the result of a combination of research projects, Complex Fracture Orthopedic Rehabilitation (COMFORT), Bone Density Analysis System (BDAS), Osteodiagnosis, and SenseBurn and is conducted by the Microwaves in Medical Engineering Group (MMG) at the Ångström Laboratory, Uppsala University. With regard to the underlying goal, clinical trials are performed with an emphasis on ethical approval, both to optimize the sensor with respect to human tissues for better accuracy and performance and to enhance the feasibility of medical diagnosis using microwaves.

With this aim in mind, the structure of this work is as follows: The first part of this work pertains to the study of the properties of different tissues (thickness, relative permittivity, and conductivity). In these Subsections 4.1 and 4.4, the efforts are invested in characterizing human tissues based on ultrasound information, and intraoperative and in-vivo measurement (**Papers I and IV**).[94–95] This work also covers clinical trials by including volunteers and patients who have undergone surgical procedures. The second part of this work covers a study protocol of clinical trials in Subsection 4.2 (**Paper II**).[113] To do so, a collaboration between medical hospitals (Uppsala Academic University Hospital, Sweden and Utrecht and Maastricht Academic University Hospital, the Netherlands) and academia (Ångström Laboratory, Uppsala University) is introduced to perform the significant clinical study related to this thesis.

In Subsection 4.3 (**Paper III)**, intensive studies are performed in regard to tissue-mimicking phantoms and ex-vivo tissue samples.[99] For this purpose, Artificial Tissue Emulating (ATE) phantoms are prepared by mixing different material compositions to create semi-solid (electrically and physically) emulating tissues. Ex-vivo measurements are conducted and tissue samples are analyzed with respect to dielectric properties of different human tissues. The final part of this work provides the extended concept of sensor development for physiological and biological properties in Subsection 4.5 (**Paper V**).[116] The highlight of the final part of this work is to investigate the variation in biological tissue thicknesses indicating a great potential application in the area of medical diagnosis.

2 Background and theory

This section gives an overview of the definitions of various medical conditions covered throughout this thesis. It also includes an important aspect of this study which is the propagation characteristics of electromagnetic (EM) signals in human tissues.

2.1 General description

This study is mainly driven by the demand for a non-invasive and non-ionizing microwave sensor-based diagnostic tool to monitor tissue variations, especially during the rehabilitation of lower extremity fractures, craniosynostosis, and burn injuries. For example, replacements ensuing bone injuries are becoming increasingly prevalent.[30] Children and the elderly have a higher tendency to suffer from bone disorders and other complications related to bone healing. This mainly affects elderly patients since they show a very high variation in the fracture healing rate. There are numerous types of bone disorders such as those developed due to osteoporosis, osteoarthritis, and non-union fractures, or surgical treatments such as to treat craniosynostosis or post-craniotomy complications such as hemorrhage, wound/soft tissue infection, and bone flap infection.[31] For burn injuries, in order to classify the degree of a burn sample, it is necessary to define a threshold for each degree of the burn. The most reliable definition of the degree of the burn can be provided by burn surgical experts.

2.1.1 Lower extremity fractures

In lower extremity trauma, musculoskeletal problems and conditions are common and the impact is pervasive.[32] This is because they have the largest and most significant impact on society and health care, and are considered as one of the most expensive disease categories.[33–35] Lower extremity fractures represent the most common cause of health problems that limits one's ability to do work and leads to early retirement or long-term sick leave. The burden of musculoskeletal conditions is predicted to increase dramatically as the age of the population increases because many of these conditions, namely osteoporosis and osteoarthritis, are more prevalent or have a greater impact on elderly people.[36–37]

Osteoporosis is described as a skeletal disease (bone disorder) that can lead to fragile bones. Osteoarthritis, on the other hand, can be classified as cartilage damage, with or without changes in interior cancellous bone, and bone marrow edema-like lesions. Because of this, the bone loses its strength which could, for instance, lead to hip replacement surgery. Osteoarthritis is the leading cause of pain and disability especially among the elderly. In Sweden, with a population of 10 million people, there are approximately 18,000 cases of hip fractures per year.[38–39] The incidence of hip fractures globally in 1990 was roughly 1.26 million and is estimated to increase to 2.6 million in 2025 and 6 million in 2050.[40–41] Considering these numbers, it is significantly important to have proper rehabilitation and to monitor the bone healing progress for healthy aging.

In lower extremity trauma, there are four different stages of fracture healing. In the first stage, a hematoma is generated after inflammation. In the second stage of the reparative period, cartilaginous tissue progressively replaces the initial fibrin and woven bone starts to form. In the third stage of the reparative phase, the cartilaginous tissue mineralizes, more bone forms, and the volume of granulation tissue substantially decreases. In the final stage, remodeling restores the original form of the bone once the bone has been bridged.[42] Figures 2.1a–d show the stages of fracture healing.

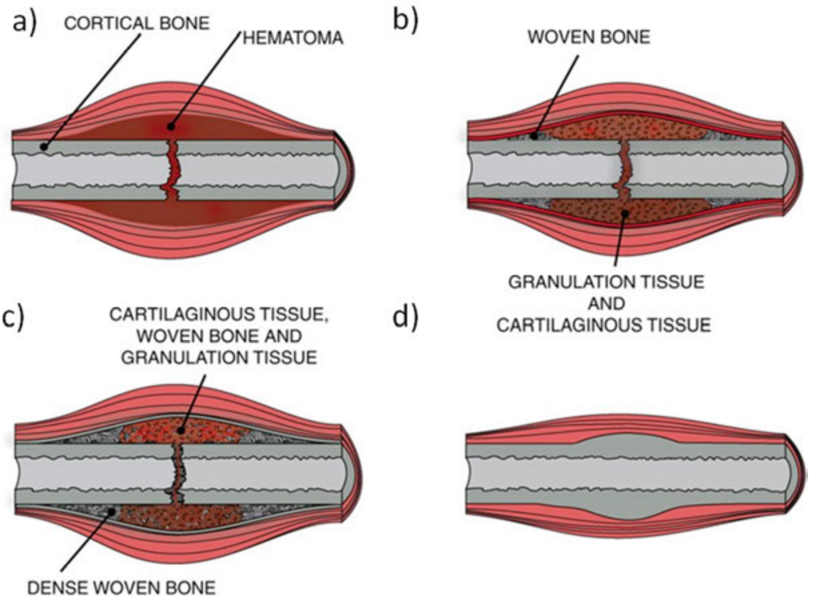

Figure 2.1 Illustration of different stages of fracture healing.[42]

2.1.2 Craniosynostosis

Craniosynostosis is a condition where the skull plates of a newborn fuse prematurely, leaving limited space for the growth of the brain. The birth prevalence of children with craniosynostosis is approximately 4 in 10,000 live births.[43] Craniotomy is a surgical intervention adopted as part of craniosynostosis treatment.[44] It is a procedure where one or a set of bone flaps are removed from the patient's skull to allow the brain to grow. Defects of different shapes and sizes, caused by the removal of bone flaps or opening the skull using spacers, form in the skull and these defects heal over time. The four main types of craniosynostosis are metopic craniosynostosis, sagittal craniosynostosis, unicoronal craniosynostosis, and lambdoid craniosynostosis, as shown in Figure 2.2.

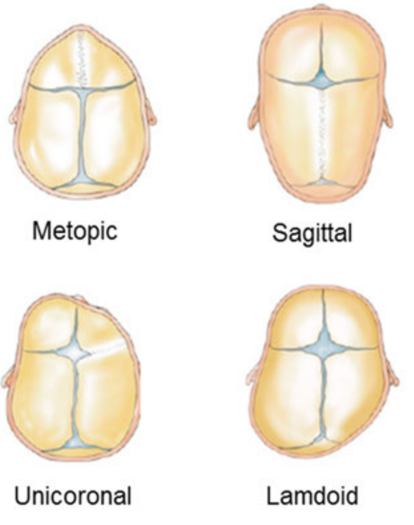

Figure 2.2 Images of cranial sutures involved in non-syndromic craniosynostosis.[45]

A summary of the intramembranous ossification steps representing the bone healing process is as follows. 1) Mesenchymal stem cells at the fracture site develop into osteoblasts which cluster together on the dura to form an ossification center. 2) The osteoblasts secrete osteoid which mineralizes after a few days. Osteoblasts trapped within the osteoid become osteocytes. 3) Trabeculae and the periosteum form. 4) The trabeculae on the external face of the bone thicken, finally forming lamellar bone. The inner part of the bone becomes cancellous, or spongy bone, complete with red bone marrow. The most important point that can be drawn from this simplified explanation is that the flat bone forms on top of the dura and subsequently grows from there.[68] These healing stages are estimated based on medical records and clinical monitoring.

Craniosynostosis has been chosen as a model since the defects made as part of its medical intervention are in the skull, and therefore close to the skin. A microwave sensor can be used in this case at low power for illuminating the defect and a penetration depth of utmost 1 cm is required. Furthermore, the operations are done in neo-natal patients and they have high growth values. Thus, craniotomy renders an ideal test environment for the clinical validation of a microwave-based bone density sensor.

2.1.3 Severe burn injuries

Burns on the surface of the body have complicated pathological impacts that can affect various functions of the body. It can occur shortly after an accident and can have serious implications on affected patients. The main causes of burn injuries include liquids, scalds, dry heat, flame, heated objects, radiation, electricity, and chemicals.[46–47] Burns are usually categorized by the depth and degree of the injury.

Table 2.1. Burn injuries classification schemes.

Classification based on the degree[50]	Classification by Derganc[48]	Classification by Shakespeare[49]
First-degree burn	Epidermal burn	Superficial burn
Second-degree burn-superficial	Dermal burn-superficial	Superficial partial-thickness burn
Second-degree burn-deep	Dermal burn-deep	Deep dermal partial-thickness burn
Third-degree burn		Full-thickness burn
Fourth-degree burn	Subdermal burn	Full-thickness burn involving underlying tissues

For the description of burn injuries, three classification schemes are currently in use as shown in Table 2.1.[48–50] Figure 2.2 shows the illustration of the classification in the degree of burn injuries where the same classification was adapted by Jaspers et al., 2016.[51,61] In this thesis, the classification by Shakespeare[49] is used to examine burn injuries in laboratory experiments and the clinical study. There are five different stages in this classification system depending on the burn depth (or thickness).[52] In the first stage, only the epidermis is affected by the burn. In the second stage, the burn affects the dermis papillary layer. In the third stage, the burn reaches the subcutaneous layer of the dermis. In the fourth stage, the burn affects the entire skin tissue whereas underlying tissues like fat, muscle, and bone are affected by the burn in the fifth stage.

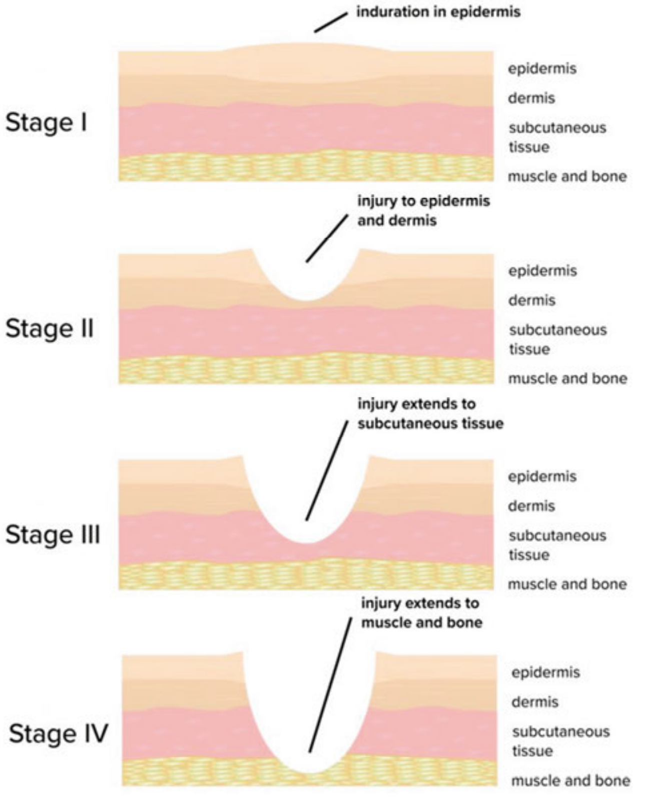

Figure 2.3 Schematic illustration of classification in degree of burn injuries.[51]

2.2 Diagnosis procedure

Diagnosis is typically done by analyzing the patient's medical history, followed by a physical examination and radiography. There are various monitoring methods available that can be used to assess fracture/defect healing in lower extremity trauma, craniosynostosis, and burn injuries.

2.2.1 Lower extremity trauma

In lower extremity trauma, radiographs are incapable of determining bone density which helps to govern bone healing and its structural integrity. Fortunately, this problem was solved with the help of dual-energy X-ray absorptiometry (DEXA) scans and QCT. DEXA helps to determine bone mineral density and bone mineral content which can be used to diagnose osteopenia and osteoporosis.[53]

Quantitative Computed Tomography (QCT), on the other hand, is based on differential absorption of ionizing radiation of calcified tissue or bone.[54] QCT is a very good indicator of the bone healing process and it eliminates the issue of overlapping structures. However, QCT is inconvenient for patients as they have to stay still during the scanning session for a prolonged duration. Moreover, QCT is high-cost, has limited availability and has a higher dose of radiation exposure compared to X-ray and DEXA scans.[54–55]

2.2.2 Craniosynostosis

Proper bone growth or transformation into bone, especially after craniosynostosis-based craniotomy, is crucial but difficult to monitor in newborn pediatric patients due to the risks associated with existing technology. X-ray examinations are more conventional, but they can only show the quantitative assessment of periosteal reactions.[56–57] It is also not sufficient for predicting the progress of healing.[58] It is difficult to correlate the estimation of bone reunion with X-ray examinations due to the formation of callus.[54] Because of this, viewing the osseous union is less reliable with X-ray readings.

2.2.3 Severe burn injuries

The assessment of burn injuries is primarily conducted by clinical evaluation. A clinical evaluation is based on visual and tactile inspections of burn wound features and it can achieve a fairly moderate precision of about 70% by experienced clinicians in the best situation.[59–60] A combination of clinical evaluation with a dependable instrument at this stage could significantly enhance the precision and make the evaluation available to less experienced clinicians. The usage of a Laser Doppler Perfusion Imaging (LDPI) tool may be the most successful method, according to the latest systematic review conducted by Jaspers et al., 2016.[61] An additional assessment reported by Jasper, 2017, uses a Forward-Looking Infrared (FLIR) tool.[50] This tool could be useful for clinicians to assess burn injuries and enable simple and fast clinical burn measurements.

2.2.4 Proposition of diagnostic tool

In this thesis, the microwave technique is presented as a possible alternative modality for bone assessment compared to QCT and standard X-ray methods. At the moment, microwave techniques have gained greater momentum in the medical field due to the development of new measurement methods, proper coupling mediums, and fast computation.[62] In addition to the current development of the microwave technique, the MMG at Uppsala University has been exploring one of these approaches. They have demonstrated the feasibility of detecting tissue variations in femur bones for osteoporosis and in skull implants [63–66], and have reported progress on the optimization of ATE phantoms and other related technologies.[67–70]

2.3 Dielectric properties of human tissues

Dielectric properties of human tissues can be defined by the level of interaction of EM waves with different mechanisms of polarization (e.g. ionic, atomic, and orientation).[71–72] The dielectric properties of human tissues are the main parameters for the numerical analysis of the propagation of EM waves in tissues. Thus, it is important to determine the dielectric properties of human tissues. The well-known Debye equation and the Cole-Cole equation will be introduced in the following Subsection 2.3.1, which can be used to predict the permittivity of human tissues based on experimental human tissue data.[73–74]

2.3.1 Debye equation and Cole-Cole equation

The dielectric properties of human tissues are frequency dependent. This can be explained by the different polarization mechanisms caused by the E-fields in human tissues.[75] Frequency-dependent behavior usually refers to the dielectric relaxation response of human tissues and can be expressed by the following Debye equation[78]:

$$\varepsilon^* = \varepsilon_\infty + \frac{\Delta\varepsilon}{1+j\omega\tau} \tag{2.1}$$

where ε^* is the complex permittivity of a medium as a function of the angular frequency, ω, ε_∞ is the permittivity at a higher frequency limit and $\Delta\varepsilon = \varepsilon_s - \varepsilon_\infty$ where ε_s is the permittivity at a lower frequency limit, τ is the relaxation time, which is the required time for a stimulated dipole to return to its original state. In the Debye equation, the term of relaxation time is regarded only as a first order and it is not sufficient to be used to determine dispersion within a broad frequency range.

This means that equations of a higher order in terms of several relaxation times must be considered to account for the multiple time constants of different mechanisms of polarization.[77] To enable this, Cole and Cole have made a commonly used modification to the Debye equation. The Cole-Cole equation provides multiple dispersion terms based on numerous reported experimental data from different tissues.[73–74, 78–80] The Cole-Cole equation can be defined as the equation below:

$$\varepsilon^* = \varepsilon_\infty + \sum_n \frac{\Delta\varepsilon_n}{1+(j\omega\tau'_n)^{(1-\alpha_n)}} + \frac{\sigma_i}{j\omega\varepsilon_0} \tag{2.2}$$

where $\Delta\varepsilon = \varepsilon_s - \varepsilon_\infty$ expresses the dispersion magnitude, α_n is the distribution parameter, n indicates four different dispersion regions, and σ_i is the static ionic conductivity of the tissue.

2.3.2 Permittivity profile of human tissues

Since lower extremity fractures, craniosynostosis, and burn injuries are within the scope of this thesis, relevant dielectric properties of different tissues are analyzed. The permittivity of various tissues can be estimated in a wideband frequency range based on the Cole-Cole equation (the frequency range in this study is between 1 and 10 GHz). Figures 2.4a–b show the relative permittivity and conductivity over frequency in cases of lower extremity fractures and burn injuries. The dielectric properties of ten types of tissues (skin dry, skin wet, fat, muscle, cortical, cancellous, cartilage, marrow, tendon, and blood) are presented. The dielectric properties of air, on the other hand, are included for comparison with the free space condition.

The tissues of fat and marrow have the lowest relative permittivity of around 5 (Figure 2.4a) since these tissues have almost negligible water content. In addition, the dispersion of the fat and marrow tissue permittivities in the frequency range from 1 to 10 GHz is not noticeable. The cortical and cancellous permittivities are then studied. At a targeted frequency of 2.45 GHz, the cortical and cancellous have a relative permittivity of 12 and 18, respectively. In contrast, blood and muscle have a higher relative permittivity of around 52 and 58, respectively, due to high water content in the tissues. Hence, the frequency dependence of the relative permittivity of tissues with high water content varies significantly from 1 to 10 GHz.

Figure 2.5b illustrates the conductivity of different human tissues and is referred to as the losses of the corresponding material. Marrow, fat, cortical, and cancellous bone exhibit low values of conductivity, while blood, muscle, and tendon show high values of conductivity. Muscle and blood have conductivities of 1.7 and 2.5 S/m at 2.45 GHz, respectively. Furthermore, a large attenuation of EM signals is predicted in muscle and blood (refer to Appendix A).

Regarding craniosynostosis, Figures 2.5a–b show the relative permittivity and conductivity of different human tissues over frequency. The dielectric properties of nine types of tissues (skin dry, skin wet, muscle, cortical (skull), cancellous, white matter, grey matter, cerebral spinal fluid (CSF), and blood) are presented. Additionally, the presence of muscle will be included in this study, since certain parts are covered by muscle tissue (e.g. frontalis muscle).

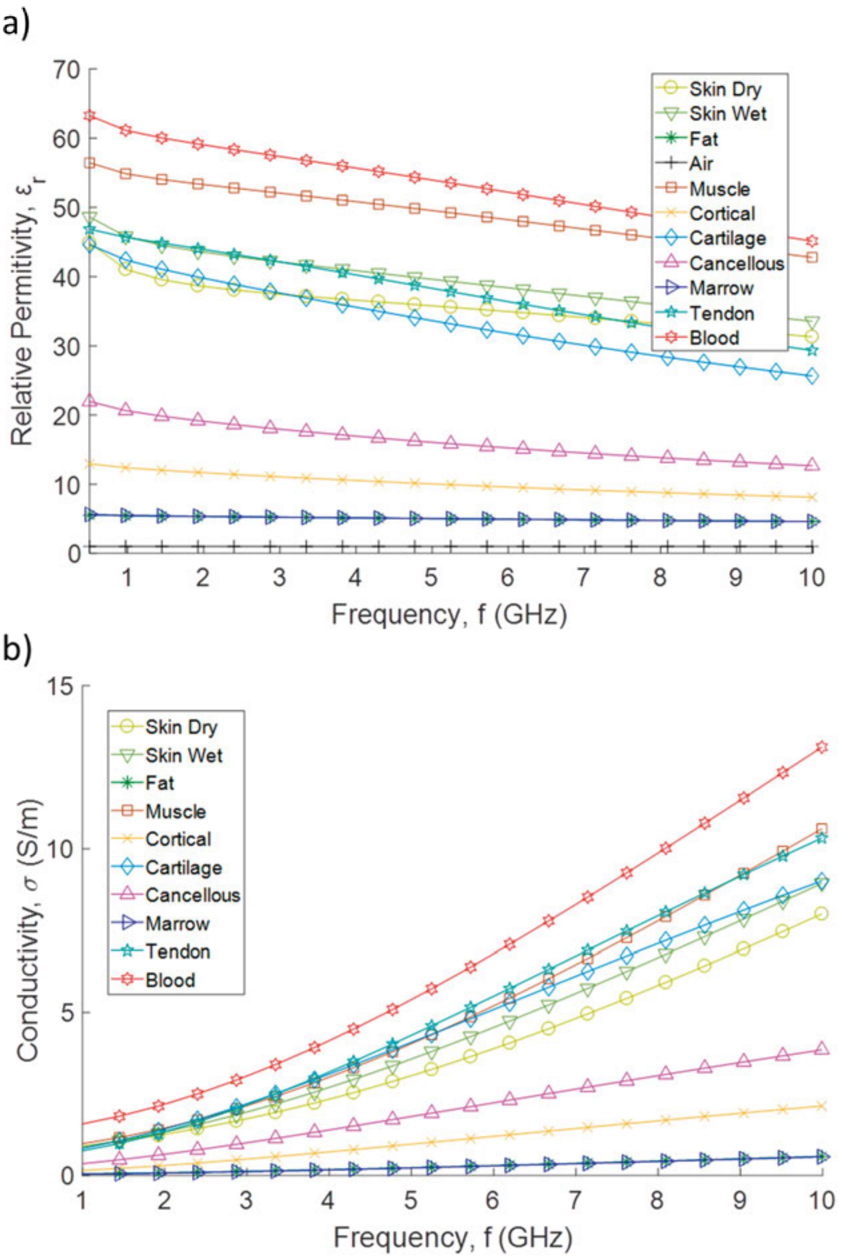

Figure 2.4 a) Relative permittivity b) Conductivity of different human tissues over frequency for lower extremity trauma and burn injuries (skin dry and skin wet).[83]

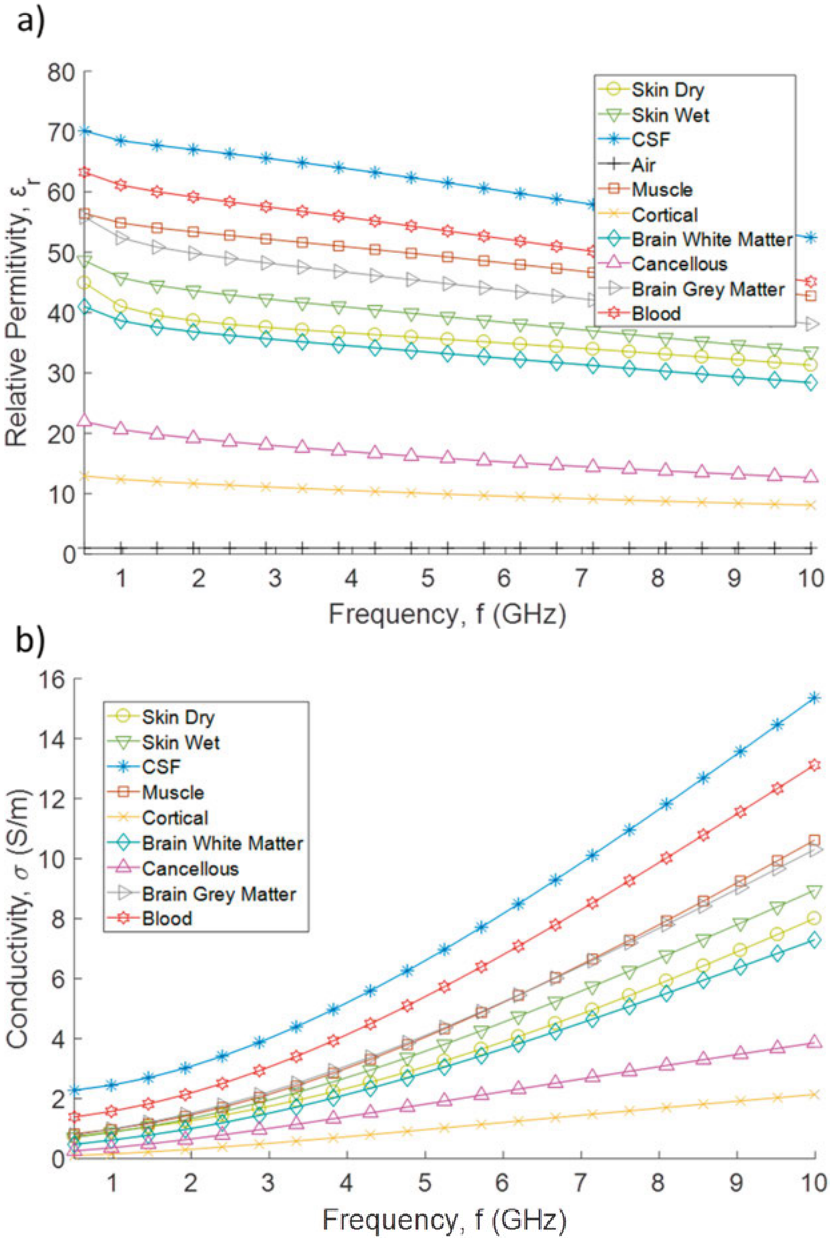

Figure 2.5 a) Relative permittivity b) Conductivity of different human tissues over frequency for craniosynostosis.[83]

From Figures 2.5a–b, it can be seen that cortical and cancellous bone have the lowest relative permittivity and conductivity (same results as in lower extremity fractures). However, CSF shows higher relative permittivity and conductivity of 66 and 3.5 S/m at 2.45 GHz, respectively. Thus, the resultant high contrast between the surrounding tissues provides the potential to detect the volume of CSF accumulation in the human body. It can also be observed that the frequency dependence on the conductivity of tissues with high water content increases slightly from 1 to 10 GHz. The conductivity of tissues with high water content increases with the frequency.

2.4 The effects of microwave propagation in the human body

The propagation characteristics will be explained in this section. Here, the dielectric properties of different tissues are investigated. The propagation characteristics of the microwave signals in human tissues are provided with respect to frequency dispersion, reflection, penetration depth, and attenuation.

2.4.1 Reflection coefficient

Reflections occur at different tissue boundaries during the propagation of microwave signals in the human body. In this case, the main focus of the human body are lower limbs and the skull which have skin, fat, muscle, and bone. Bone is not one homogenous tissue, but it is composed of different parts, specifically cortical and cancellous bone, cartilage, and bone marrow.

The magnitude of microwave signals depends on the dielectric tissue contrast. The normalized reflection coefficient can be defined as:

$$\Gamma = \frac{\sqrt{\varepsilon_1}-\sqrt{\varepsilon_2}}{\sqrt{\varepsilon_1}+\sqrt{\varepsilon_2}} \tag{2.3}$$

where ε_1 and ε_2 are the permittivities of the two dielectrics of different tissues. As shown in Figure 2.6, microwave signals propagating through the multilayer human body will experience reflections on the boundaries between different tissues. The boundaries between air and skin will have a strong reflection and half of the energy is reflected back. As the contrasts between skin and fat as well as between fat and muscle are very high, these two boundaries will have strong reflections.

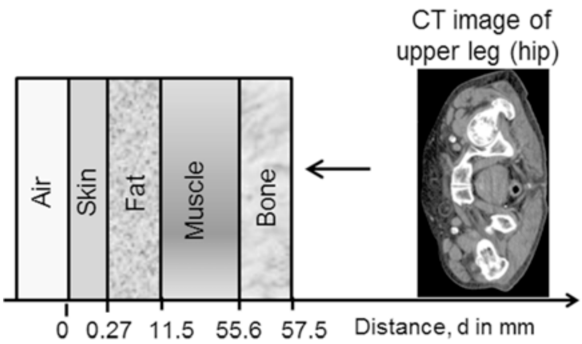

Figure 2.6 Multilayer tissues of human lower leg obtained from CT images.

2.4.2 Penetration depth

Penetration depth can be described as the ability of EM waves to penetrate a lossy medium (in this case, the focus is human tissues). The electric (E) and magnetic (H) fields inside the tissue at radio frequencies decrease exponentially as the distance from the boundary of a tissue increases because energy dissipates after reflection occurs.[82] Penetration depth is a function of frequency and dielectric properties of the tissues and it can be expressed as:

$$\delta_p = \frac{c}{\omega\sqrt{\frac{\varepsilon_r}{2}\left[\sqrt{1+\left(\frac{\sigma}{\omega\varepsilon_0\varepsilon_r}\right)^2}-1\right]}} \tag{2.4}$$

where $\omega = 2\pi f$ is the angular frequency and *f* is the frequency. ε_0 and ε_r are the permittivity of free space and the relative permittivity of a lossy medium, respectively. c is the speed of light which is 3×10^8 m/s and σ is the conductivity of the medium.

The fields penetrate much less at higher frequencies than at lower frequencies. For instance, at 2.45 GHz (microwave frequency range), the tissue penetration depth is about 2.0 cm, while at 10 GHz, the penetration depth is about 0.4 cm.[83] At frequencies between 300 MHz and 3000 MHz, EM energy can deeply penetrate tissues, making it particularly suitable for therapeutic applications.[83]

2.4.3 Attenuation

Attenuation can be defined as the loss of wave amplitude due to several mechanisms such as the impacts of scattering and absorption and mode conversion. The loss of the incident wave on a medium is characterized by its attenuation coefficient which can be described as:

$$\alpha = \frac{\omega}{c}\sqrt{\frac{\varepsilon'}{2}\sqrt{1+(\tan^2\delta)}-1} \qquad (2.5)$$

where,

$$\tan\delta = \frac{\varepsilon''}{\varepsilon'} = \frac{\sigma}{\omega\varepsilon_0\varepsilon_r'} \qquad (2.6)$$

where α is the attenuation coefficient, ω is the angular frequency, ε' is the real part of the permittivity, ε'' is the imaginary part of permittivity, δ is the dielectric loss angle, c is the speed of light, σ is conductivity of the medium, and ε_0 is the permittivity of free space.

2.5 Measurement methods of dielectric properties

Several methods can be used to measure the dielectric properties of human tissues such as resonators cavity perturbations, open-ended coaxial, and transmission line probe methods. The most commonly used among these methods are the open-ended and resonant probe methods.[73–74, 84–85]

2.5.1 Open-ended coaxial probe method

An open-ended coaxial probe comprises a cut-off segment of a transmission line. The material is measured by submerging the probe into a liquid to make the probe to have sufficient contact with the surface of a semi-solid material. The EM field propagates along the coaxial line towards the material. Reflection occurs when the EM field experiences an impedance mismatch between the probe and the material under test (MUT). Figures 2.7a–b show the schematic illustration of an open-ended coaxial probe cross-section and an experimental setup.

The reflected signals are measured at different ranges of frequencies and then converted into complex permittivity, a process usually done automatically by using integrated software in the Vector Network Analyzer (VNA).[86] This method is frequently used to measure tissue permittivity. It has several advantages as it is non-destructive, simple, and convenient and it has a broad frequency range that is suitable for ex-vivo and in-vivo measurements. However, this method requires sufficient contact between the probe and homogeneous samples. Otherwise, an irregular surface and air gaps in the samples will generate inaccurate measurements.[87]

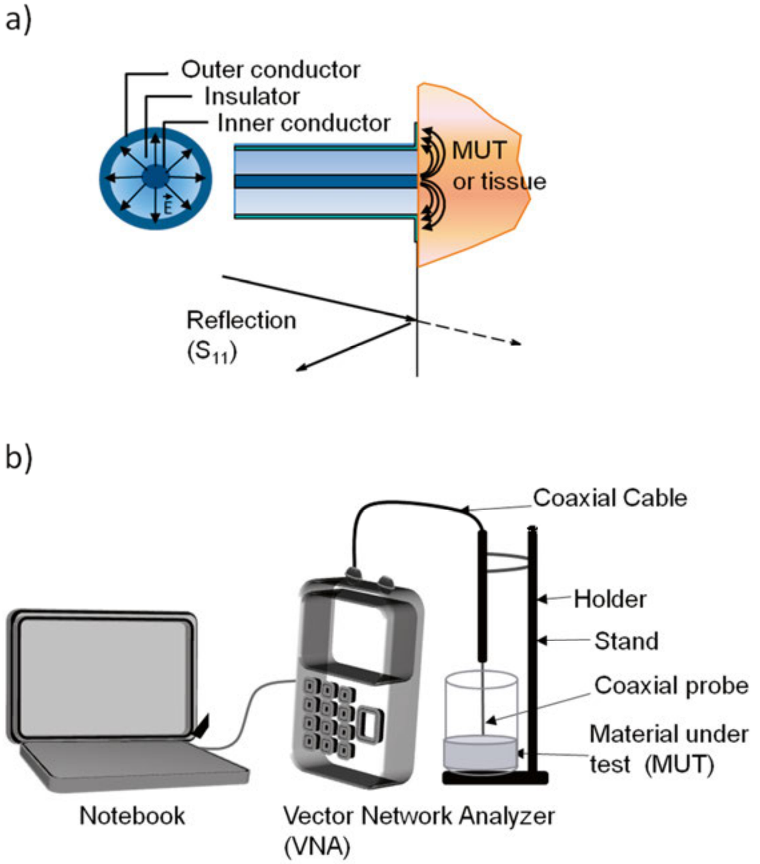

Figure 2.7 Schematic illustration of a) top and cross-section view of the coaxial probe and b) measurement setup consisting of Vector Network Analyzer (VNA), coaxial cable, coaxial probe, and material under test.

2.5.2 Resonant probe method

There is a considerable number of microwave resonant-perturbation methods applied in different fields of material characterization using electromagnetic devices. Existing literatures offer several types of resonator probe methods that could be considered for material characterization: coaxial-tip, open-coaxial, metallic waveguide, dielectric, and microstrip methods.[88–92] However, one type has recently been studied in its preliminary stages on the clinical study of bone defects.[66] This type consists of a proximity coupled split ring resonator (Figure 2.8) which will be widely covered in the entire thesis from laboratory to clinical trial setups. Therefore, details of the other resonator probe methods are not discussed in detail here, but more data can be discovered in.[88–92]

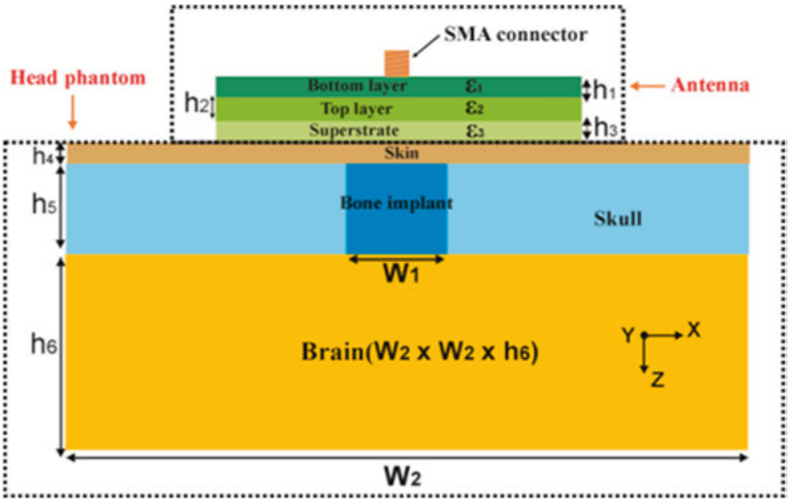

Figure 2.8 Illustration of proximity coupled split ring resonator attached to the head phantom in the case of craniosynostosis. Here, the antenna is based on the SRR structure and applied directly to skin surface.[66]

The proximity coupled sensor comprises a highly directive microwave split ring resonator (SRR) with a small form factor placed directly on the areas of interest (in this case, the bone defect). The resonance frequency of the probe is highly dependent on the effective permittivity of the surrounding area. The radiation properties of the probe are not analyzed. Instead, the dispersive effect regarding the dielectric properties of human tissues is studied. Since the measurements will be done in the frequency domain, the probe should have a good impedance matching to the body and a narrow bandwidth to distinguish shifts in resonance frequency when placed above the areas of interest.

2.5.3 Phantoms of the human body

Before moving on to clinical trials on humans, there is a need for an ATE phantom in order to verify the development of the probe. The ATE phantom has electrical properties that closely emulate those of human tissues across the frequency band of interest. Nowadays, there are numerous types of phantoms that have been developed, but there are three basic constructions involved such as liquid, semi-solid (gel), and solid (dry). The specific material required to create semi-solid, and electrically and physically emulating tissues is presented in **Paper IV** (for the case of craniosynostosis).

In the clinical context of this thesis, there is a necessity for a systematic way of developing realistic and anatomical phantoms that are suitable for validating microwave systems. To that end, the fabrication of a range of realistic phantoms that emulate the electrical properties of all types of healthy human tissues (specifically in lower extremity trauma, craniosynostosis, and burn injuries) over the frequency band of 1 to 10 GHz is done. This frequency band is selected because it includes bands that offer a reasonable compromise between the acceptable sensing resolution and the required penetration of low-power microwave signals.[93] The dielectric properties of different tissues are measured in terms of intraoperative measurements to compare with available literature data.[73–74,78,80] The sizes, shapes, and depths of reference and defects are characterized based on pre-surgical and post-surgical planning, and this information is included in the phantom fabrication topic.

3 Materials and Methods

3.1 Design aspect

The microwave based-sensor is one method among numerous other resonant probe methods and is extremely attractive. It is favored for being highly sensitive, small in size, has low fabrication and measurement costs, and is a non-invasive method. Important sensor specifications that are considered during the design for this thesis are the following: high directivity, has a good impedance matching to the body, and a narrow bandwidth to distinguish shifts in resonance frequency when placed above the areas of interest. The microwave based-sensor should be compact and very comfortable to be used as a proposed tool. The presented geometrical dimensions are highly optimized to have the peak performance in the 2.4 GHz Industrial, Scientific and Medical (ISM) band which is free to use.

3.1.1 The proposition of microwave sensors

The microwave sensor prototypes were simulated in Computer Simulation Technology (CST Studio, 2018, SIMULIA, Dassault Systèmes, France) and optimized and validated for human body tissues for different health conditions. The dielectric data for various tissues such as fat, muscle, skin, brain, and bone were used as initial tissue properties for the training (iteration) of the numerical model, as documented in the literature.[73–74, 80–81] Three different sensor types were developed to be used for several purposes to study various health conditions. All developed sensors are non-invasive with superficial contact to the skin surface. The analysis was made in the frequency domain and the sensor should have the best matching for skin contact compared to when observed in free space. The concept is to have a clear difference between healthy body tissues and affected tissues due to any medical condition. Consequently, high-frequency (HF) shift (resolution) can occur which helps in monitoring the healing progress.

3.1.2 Simulation design

Two types of feed techniques to couple the signal to the split ring resonator were simulated. The first uses the T-shape feedline (Figure 3.1) and another one the capacitive feed (Figure 3.2). Both (simulation) designs contain the split ring resonator structure as a key component inspired by the metamaterial structure. The simulated three-layer planar structure comprises a ring resonator, a feeding layer, and a superstrate which acts as a contact layer (**Paper I** and **Paper IV** for detailed specifications).[94–95] More energy is radiated into the human tissue with the help of the superstrate. The superstrate also illuminates the target tissues and gives rise to stable and improved resonance characteristics.

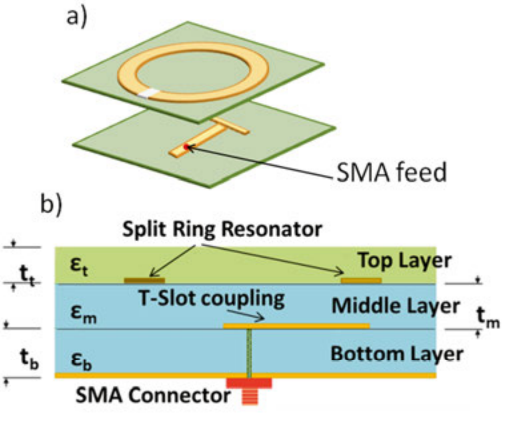

Figure 3.1 Microwave split ring resonator sensor with a T-shape feedline.

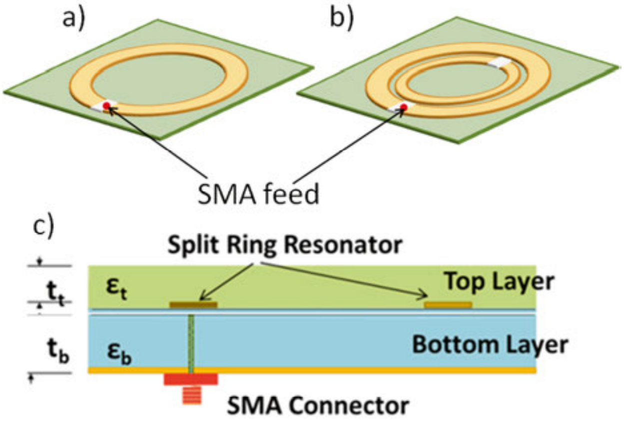

Figure 3.2 Microwave split ring resonator sensor with a capacitive feed. a) Single split ring resonator. b) Double split ring resonator. c) Side view of the proposed multilayer sensor. © 2018 Sensors. Reprinted, with permission, from [Mohd Shah, S.R., Velander, J., Mathur, P., et al. Split-ring resonator sensor penetration depth assessment using in vivo microwave reflectivity and ultrasound measurements for lower extremity trauma rehabilitation, Sensors, Feb. 2018].[94]

3.2 Fabrication process

In this work, the microwave split ring resonators (SRR) were fabricated on two types of substrates. The first type of substrate used layers of high-frequency copper clad laminates (CCL) which is suitable for rigid structures and it was fabricated using standard etching process technology. The second type of substrate used polydimethylsiloxane (PDMS) and copper sheets. The description of the entire process flow to fabricate the SRRs can be found in Subsections 3.2.1 and 3.2.2.

3.2.1 Rigid sensors

The fabrication process of the microwave SRRs involves three fundamental stages which are ultraviolet (UV) exposure, developing process, and etching process. During the UV exposure stage, the image of the layout pattern was transferred onto the photoresist laminated board with an overhead (OH) plastic film by using a UV exposure machine (Figures 3.3a–b). This process normally takes two minutes. Gerber Viewer software was utilized to transfer the geometrical shape onto a transparent plastic film. This software helps to ensure that the simulated sensors are easily transferred onto the OH plastic film according to their actual sizes.

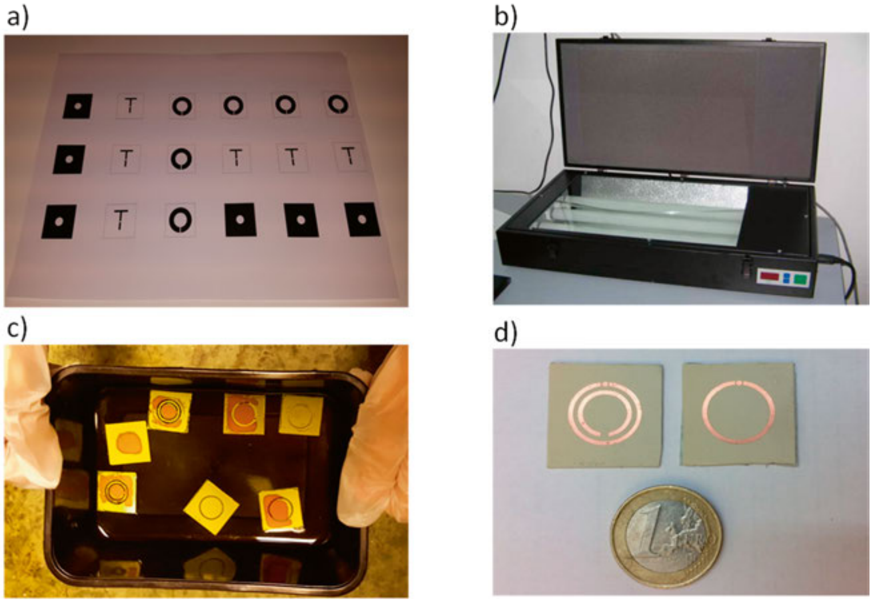

Figure 3.3 The fabrication process of a split ring resonator using the etching technique. a) Printed layers on an OH plastic film. b) UV exposure machine used to illuminate the pattern onto the substrate board. c) Etching process with $FeCl_3$ to remove the unwanted copper area. d) Fabricated split ring resonator sensors.

In the developing stage, the substrate was dipped into a sodium hydroxide solution for about 45 seconds to a minute until the image developed. The developer washed away the photoresist layer that was exposed to UV light. As a result, the photoresist formed a protective layer over the layout pattern and left the rest of the copper area exposed. Then, the substrate was rinsed with tap water, revealing the image of the patch which was covered by a clear dark yellow layer of photoresist.

The last stage in the fabrication of the microwave SRRs is the etching process. Ferric Chloride ($FeCl_3$) developer was used to etch out the layout pattern as illustrated in Figure 3.3c. This process usually takes 10 minutes.

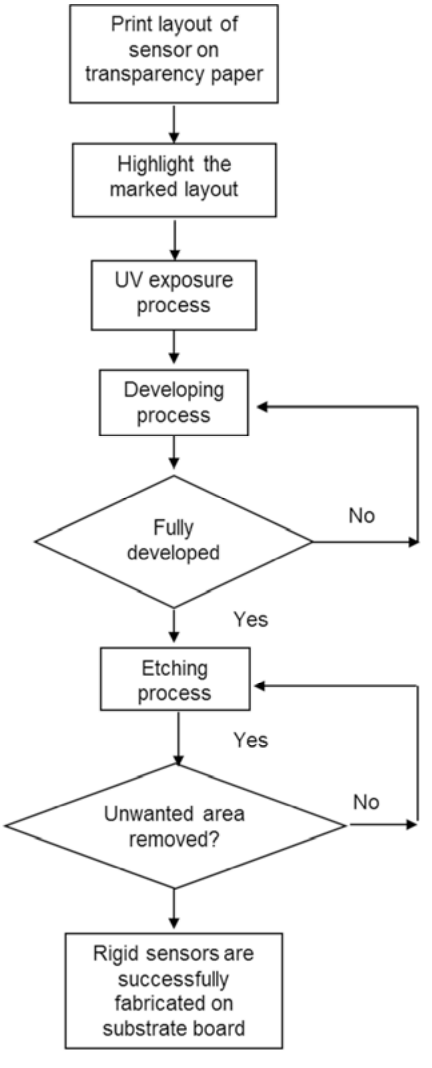

Figure 3.4 Flow chart of the etching process.

After the layout was etched out, the sensor was washed in tap water and then dried (Figure 3.3d). The outer part of a SubMiniature version A (SMA) connector was soldered to the ground plane layer and a feeding pin was connected to the microstrip feed and measured to make sure that it did not short-circuit. All layers were then stacked and glued together using adhesive glue. A complete flow chart of the etching process is shown in Figure 3.4.

3.2.2 Flexible sensors

The fabrication process to develop flexible SRR sensors from the PDMS substrate was proposed by Abbas et al., 2018, and is illustrated in Figures 3.5a–d.[96] The PDMS components Wacker Silicones Elastosil RT 601 A (monomer) and RT 601 B (curing agents) were used in the fabrication process.[97–98] PDMS was selected because of its mechanical stability, flexibility, water resistance, and inertness. The PDMS substrate was made manually by using the monomer and the curing agents in a ratio of 9:1. The fabricated PDMS substrate was used to laminate the copper sheet-SRR pattern and the desired substrate thickness was set using custom-made molds.

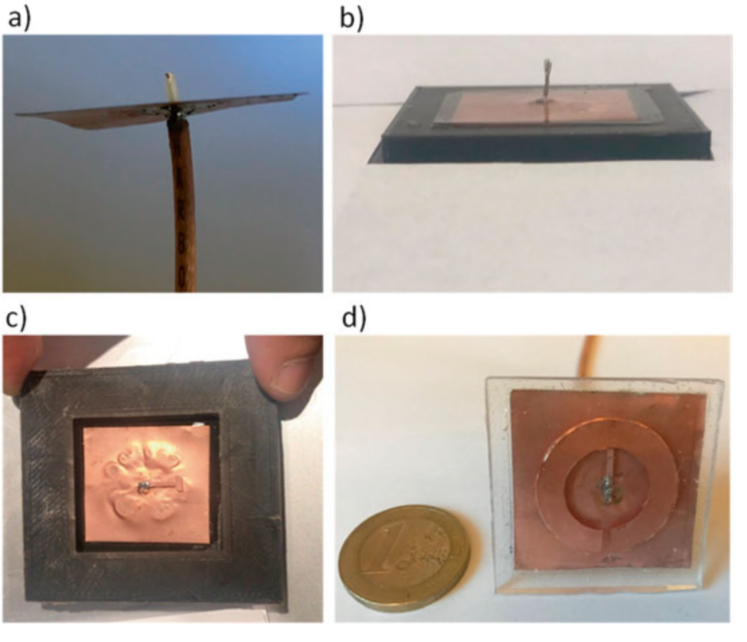

Figure 3.5 The fabrication process of the PDMS microwave sensors, patterned with the copper sheet-SRR pattern. a) Ground plate was connected to the coaxial cable. b) The first dielectric PDMS layer was laminated on the ground plate using custom-made 3D-printed molds. c) The T-shape was patterned with the same process as the ground plate and the dielectric PDMS layer was laminated with the same process as the first substrate. d) Final fabricated PDMS split ring resonator sensors.

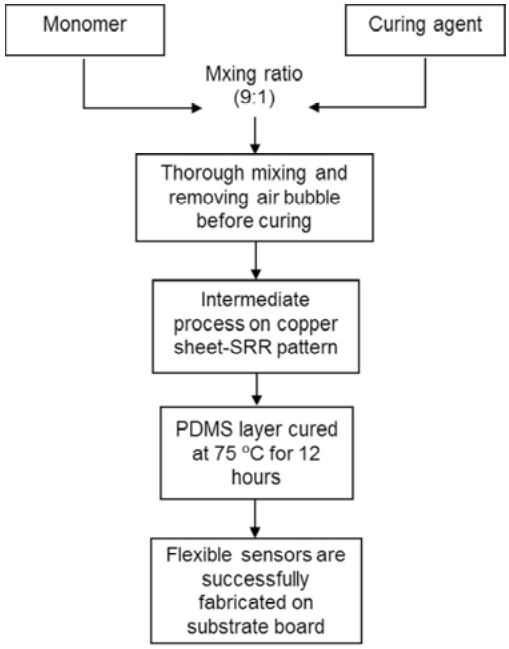

Figure 3.6 Flow chart of the PDMS substrate fabrication process.

Every PDMS layer was semi-cured at 75 °C for a certain time depending on the thickness of the PDMS layer. This was made to create a good bond between the layers and to ensure good wetting ability of the copper sheet-SRR pattern. After the fabrication of all the layers, the whole structure was fully cured at 75° C for 12 hours.[99] The thicknesses of the PDMS layers were about 5 mm.

3.3 Measurement setup

The Microwaves in Medical Engineering Group (MMG) at Uppsala University intensively runs both laboratory and clinical measurements in Sweden and the Netherlands. At the time of this study, in-vivo measurements are performed both invasive and non-invasive for different research purposes and are still being carried out to this day. Invasive measurements are mainly performed to have a better understanding of each body tissue in a living human. Invasive dielectric characterization measurements are done during craniotomy and hip replacement surgeries. Non-invasive measurements are done on healthy volunteers and patients undergoing rehabilitation for craniotomy and hip fracture surgeries. This thesis includes the study protocol for lower extremity injuries in proximal femur fracture treatments in elderly patients. Ethical approval is granted for craniotomy measurements on younger children suffering from craniosynostosis. This facilitates clinical follow-up measurements for the development of the sensors as new data obtained from intraoperative measurements used for dielectric characterization measurements can be compared with available data from existing literature. Intraoperative measurements are done during hip replacement surgeries on patients suffering from osteoporosis. In this case, skin, fat, muscle, tendon, and bone such as cartilage, cortical and marrow tissues are examined.

3.3.1 Laboratory measurement

In this study, the tissue properties were measured by using a Keysight dielectric probe connected to a Keysight FieldFox Network Analyzer N9918A in combination with a Keysight (Agilent) 85070E Dielectric Probe Kit.[100–101, 86] The Keysight dielectric probe was constructed from a semi-rigid coaxial cable (RG-405) with a standard diameter of 2.4 mm having a center conductor and an insulator of 0.62 mm and 1.78 mm in diameters, respectively. The insulator material was assumed to be teflon ($\varepsilon_r = 2.1$, $\sigma = 1\times10^{-23}$ S/m) while the conductor material was assumed to be nickel ($\varepsilon_r = 1$, $\sigma = 1.43\times10^{7}$ S/m) in this study.

In this setup, the probe was held in place by attaching it to a grip-stand while the other components were not, to minimize both cable movement and repeatable errors. The probe was calibrated using a three-load standard calibration: in open air, connected to a shorting block, and immersed in deionized water at 22 ºC. After each individual calibration, the system performance was validated by measuring the dielectric properties of a standard reference liquid which was deionized water. The temperatures of the calibration and validation liquids were noted during each dielectric measurement. The relative permittivity and conductivity were calculated over a microwave frequency range of 0.5 to 10 GHz for each tissue/liquid measurement.

Following the laboratory setup, this work has also been previously done using Anthropomorphic Tissue Emulating (ATE) phantoms. Data on the composition of individual tissues and their thicknesses acquired from ultrasound and CT scan images can be seen in **Paper I** and **Paper IV**. The dielectric properties of various tissues were taken from an online source on the dielectric properties of body tissues, Nello Carrara-Florence (Italy).[83] The real part of relative permittivity, ε_r, and conductivity, σ, expressed in S/m were taken into consideration for the dielectric properties of the individual tissues.

The first step was to find the right materials to build semi-solid ATE phantoms that electrically and physically emulate human soft tissues. Different materials were used in the fabrication process of craniotomy phantoms such as agar, polyethylene powder (PEP) with a particle size of 25 mm, calcium sulfate, TX-151, sodium chloride, gypsum, deionized (DI) water, and gelatin.[102] Agar is used to maintain the desired shape of the phantom and to ensure that it does not influence the relative permittivity. PEP is also used to ensure that the permittivity is within control as its addition decreases the real part of the relative permittivity. Calcium sulfate is used as it has similar physical properties to the human skull such as hardness and it can be used to create and imitate defects in the skull. TX-151 is used to increase the viscosity of the phantom. To ensure that the conductivity of all phantoms is similar to the realistic tissue of the skull, sodium chloride is used. These materials are easy to use, non-toxic, and low cost. We obtained exceptional results for the relative permittivity, $\varepsilon_{r,}$ and loss tangent (tan δ) similar to that of real human tissues by selecting the correct amount and proportion of each material.

3.3.2 In-vivo and ex-vivo measurements

For the characterization of the dielectric properties of the tissues, the dielectric probe in the aforementioned subsection was used for in-vivo and ex-vivo measurements. The probe has a diameter of 2.4 mm and a length of 200 mm and it can be autoclaved until 125 ºC.

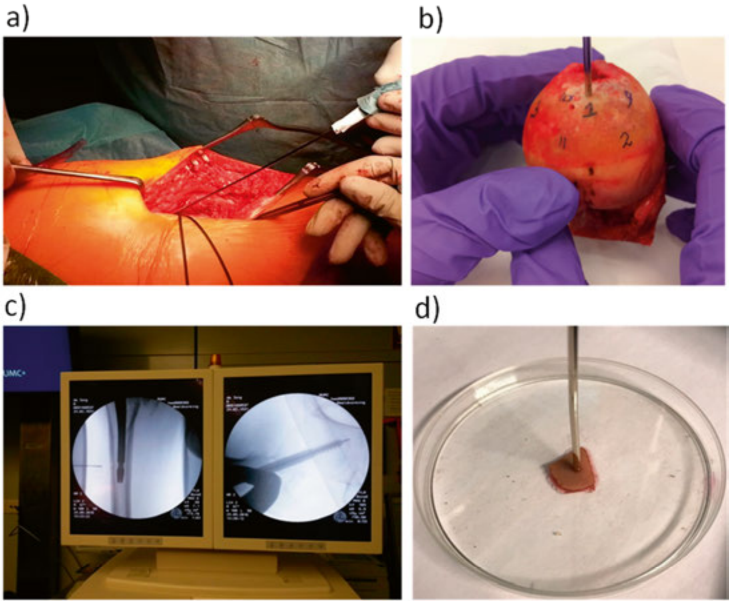

Figure 3.7 Photographs of the intraoperative and ex-vivo measurements to characterize human tissue dielectric properties. a) Dielectric probe used during surgery in the operation room. b) Ex-vivo measurement on the femoral head of a hip fracture. c) Ultrasound images of the dielectric probe inside the femur bone. d) Ex-vivo measurement on the skull bone with craniosynostosis.

A medical autoclave is a device used in hospitals for the sterilization of surgical tools. The sterilization process is a standard requirement and has to be performed during intraoperative measurements. The in-vivo and ex-vivo measurements involved skin (wet and dry), fat, muscle, tendon, blood, cartilage bone, cortical bone, trabecular bone, bone marrow, skull, and scalp. The dielectric properties of the tissues and their compositions were obtained from patients with lower extremity injuries and craniosynostosis and are shown in Figure 3.7. The measurements were taken at Maastricht Medical University Center (MMUC), the Netherlands, involving elderly patients with lower extremity injuries and at Akademiska Sjukhuset Uppsala, Sweden, involving infants who were treated for craniosynostosis through craniotomy surgery.[95]

3.3.3 Clinical measurement

A complete microwave sensor Bone Density Analyzer (BDA) system, as shown in Figure 3.8, was adapted for the monitoring of medical conditions such as lower extremity injuries and craniosynostosis. The microwave sensor system consists of a range of sensors (as described in Subsection 3.1.2) optimized for different medical conditions, a mini-VNA* to send and receive microwave/RF signals, and a personal computer (PC)/smartphone-based user interface to compute the bone mineral density based on the differences between the transmitted and received signals.

The resonance frequencies of the microwave sensors are highly dependent on the effective dielectric constant of the encompassing regions. If the microwave sensor is highly capable of detecting the dielectric variation around it, then it has high potential to be used as a non-invasive microwave healing diagnosis device.

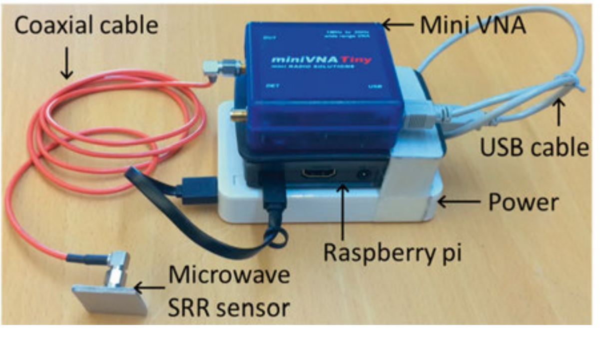

Figure 3.8 The complete setup of a microwave sensor Bone Density Analyzer system diagnostic tool prototype. © 2019 Sensors. Reprinted, with permission, from [Mohd Shah, S. R., et al. Microwave-sensor-based clinical measurements for monitoring post-craniotomy bone development in pediatric craniosynostosis patients, Sensors, 2019].[95]

---

* The microwave sensors were connected to the Mini Vector Network Analyzer, mini-VNA (mini Radio Solutions, 2014, WiMo Antennen und Elektronik GmbH, Herxheim, Germany) which operates at a frequency range of 0.001 to 3 GHz.[103]

3.4 Clinical studies

Clinical data was gathered according to ethical approval which was already sanctioned to be used for clinical trials. The ethical approval are attached to this study in Appendices B–D for the cases of lower extremity injuries, craniosynostosis, and burn injuries.

3.4.1 Proximal femur fracture

As this study focuses on human subjects, a standard study protocol is necessary. The first aim of this study protocol trial is to study the typical gait patterns of the elderly after experiencing proximal femur fractures. This study protocol is an international and multicenter trial carried out in the Netherlands and Sweden between March 2017 and August 2018 and is guided by the SPIRIT (Standard Protocol Items: Recommendations for Interventional Trials) Statement (refer to supplementary file in **Paper II**).[113] The study rehabilitation centers focusing on geriatric rehabilitation were asked to participate in this study. A minimum of 20 patients as prospective subjects are required every year to ensure the quality and expertise of the participating centers. Qualified patients are also screened at each center before they participated in the study. Ethical approval was obtained prior to start of the study (Appendix B).

Trained physical therapists who took measurements were required to have experience in geriatric trauma care. Before conducting the study, all physical therapists agreed on the study treatment regime after numerous consensus meetings and were trained to execute the study treatment regime in a uniform manner. This study protocol will contribute to existing knowledge in the rehabilitation of hip fracture patients, specifically the elderly. It is also hoped that the study will play a part in providing an improved outcome for those who are affected.

Multiple microwave sensors for BDA system were selected to be used to validate measurement at the distal, the thigh region, and at the height of the greatere trochanter (the proximal femur). The same microwave sensor system described in Subsection 3.3.3 has been used for lower extremity injuries at rehabilitation centers in the Netherlands and Sweden (Figure 3.9a). The positioning of sensors in each area of measurement was carried out in such a way that no air gap or disturbances should affect the area. This was performed with the help of a strap or band which was wrapped around the area along with the sensor (Figure 3.9b).

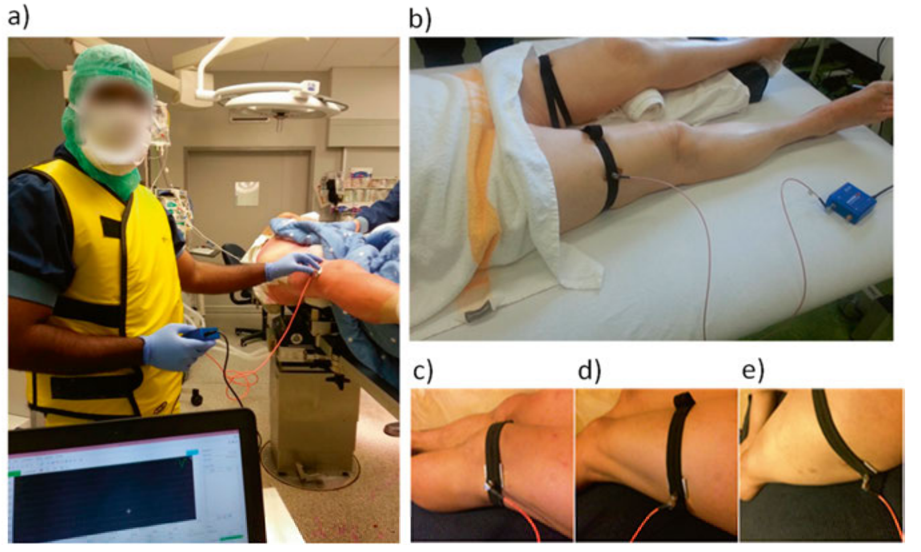

Figure 3.9 a) Clinical trial of a microwave sensor system in an operation room at Maastricht University Medical Center. b) The measurements were obtained from the thigh position on a lower extremity trauma patient. Microwave sensors were fitted to the leg using elastic bands on the c) distal d) thigh and e) trochanter. © 2018 Sensors. Reprinted, with permission, from [Mohd Shah, S.R., Velander, J., Mathur, P., et al. Split-ring resonator sensor penetration depth assessment using in vivo microwave reflectivity and ultrasound measurements for lower extremity trauma rehabilitation, Sensors, Feb. 2018].[94]

Three different sensors were made; each sensor was optimized for the physiological conditions of the intended location of use on the femur (Figures 3.9c–e). The implementation of this sensor is useful for the continuous diagnosis of lower extremities. The BDA and ultrasound were used in this clinical trial campaign. Both analyses were conducted in the Telge Rehab Center, Sweden. Apart from that, the position of the femur was fixed for each BDA measurement and at the same time, ultrasound images were obtained. The ultrasound measurement was performed to validate the tissue thickness for each layer (skin, fat, muscle, and bone) and to compare with the BDA measurement.

3.4.2 Craniosynostosis clinical trial

In craniosynostosis (**Paper IV**), 20 children with craniosynostosis treated at Craniofacial Center, Uppsala University Hospital were subjected to a series of clinical studies.

Measurements were performed postoperatively at a number of occasions on the operating table with the anesthetized patient (Figures 3.10a–c), on the discharge day which is 1 week after surgery (Figure 3.10d), the healing control during the 1-month post-surgery reception, (Figure 3.10e) in the 3rd and 6th month after surgery in conjunction with home visits, and 12 months after surgery by visiting the clinic. Figure 3.11 shows various time points when the clinical measurements were administered, starting with baseline measurements carried out pre-operatively on the operating table with the anesthetized patient.

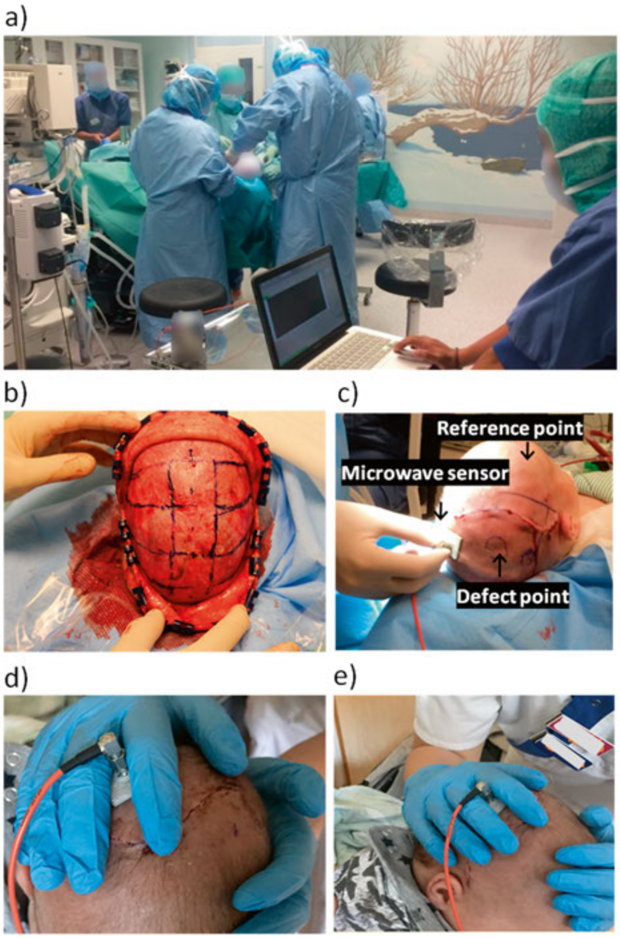

Figure 3.10 a) Proposed diagnostic tool prototype in a clinical test in the operating theatre of Craniofacial Center, Uppsala University Hospital. b) Superior view of the fetal skull of a patient undergoing sagittal craniosynostosis surgery. c) Location of measurement points (reference and possible defect locations) on a newborn's head. Follow-up clinical measurements were carried out with the help of a craniofacial nurse. d) 1-week follow-up measurement after surgery. e) 1-month follow-up measurement after surgery. © 2019 Sensors. Reprinted, with permission, from [Mohd Shah, S. R., et al. Microwave-sensor-based clinical measurements for monitoring post-craniotomy bone development in pediatric craniosynostosis patients, Sensors, 2019].[95]

Measurement data are related to the images made by the patient's skull CT scan before surgery and 1 year after surgery according to the clinical routine. Data generated by the sensors were further processed to extract mineralization data.[95, 104–107] The measurements are normally taken on various parts of the head which includes one or a few measurements on the defects and a reference measurement on the area of the forehead.

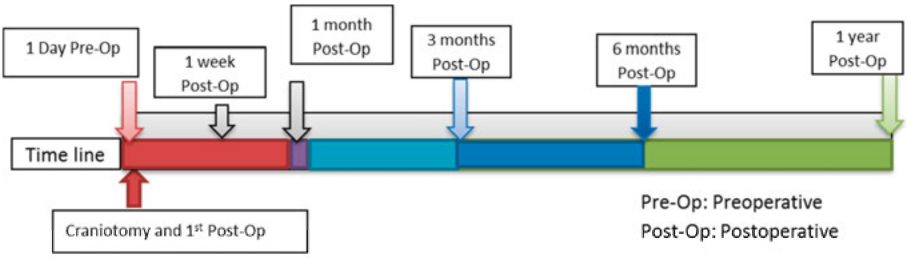

Figure 3.11 Clinical trial timeline for craniosynostosis.

3.4.3 Assessment of the depth of burn injuries

Burns are common among children and adults. The Burn Center at Uppsala University Hospital is one of Sweden's two national centers for severe burns. The bases of treating all burns are to estimate the burned body area (% of total body surface area burned, TBSA%) and to ascertain the burn depth. These two parameters determine the severity of the injury and subsequently the level of care the patient requires. It also constitutes an "outcome" predictor, i.e. the patient's functional level after treatment.

The depth of burns was previously referred to as first-degree, second-degree and third-degree burns, but modern terminology now refers to burns as superficial, superficial dermal, deep dermal (more severe scalds or flame/contact burns), and full-thickness (severe flame burns). The assessment of the extent and depth of burns is primarily done by performing a clinical assessment.

Consecutive patients admitted to the Department of Plastic and Maxillofacial Surgery at Uppsala University Hospital are approached for informed consent if they fulfill all inclusion criteria. Patients undergoing routine (plastic) surgery involving the removal of healthy skin are asked for permission for their skin samples to be transported to the laboratory, instead of having it discarded in the operating room. The skin samples are used as control tissues and are measured with a probe and a sensor after which the skin is discarded.

Patients undergoing burn surgery involving the removal of burned tissue/skin are also asked for permission for their tissue samples to be transported to the Ångström Laboratory to be measured with a probe, instead of having it discarded in the operating room. Tissue samples are then sent for histological processing, staining, and assessment, followed by the discarding of the samples. All tissue samples are sent to the laboratory unidentified.

Probe measurements are performed according to the local protocol, i.e. the tissue is put on a bench and a probe is inserted into the tissue and readings are recorded. Normal skin is discarded. For burned tissues, the area measured with the probe is cut, labeled, and put in formaldehyde for fixation after which the samples are sent to histology. For histological assessments, the samples are handled according to the routine protocol for processing and staining of the histological samples. After proper staining, the histological sections are assessed with a light microscope and the depth of the burn is categorized as a superficial, superficial dermal, deep dermal or full-thickness burn.

3.4.4 Ex-vivo human (burnt) skin samples

The H2020 Eureka Eurostars SenseBurn consortium conducts a clinical trial campaign in Uppsala University Hospital's Burn Center (Sweden) to collect human tissue samples (surgical waste) of different burn depths, from full-thickness to superficial burns. After obtaining informed consent, samples are collected in the hospital's operation room during necrosectomy of acute burns and placed in sterile jars and refrigerated while waiting to be transported to the Ångström Laboratory, Uppsala University, for microwave dielectric permittivity together with the clinical assessment of the burn depth.

In this clinical study, normal skin was measured to obtain reference values for human skin and burned tissue was measured to calibrate it to measure the correct burn depth. Both sample tissues were measured using the dielectric probe, as shown in Figures 3.12a–b. Samples were divided into homogeneous sectors and the dielectric profiles at microwave frequencies were measured at these sectors (Figure 3.12c). The sectors consist of different measurement points (repetitions) for a better homogenization of reported values. The measured dielectric profiles were compared to those reported in existing literatures which are the standard deviation to consider the accuracy of the measurements.[73–74,78,80]

After the probe measurement, the tissue was sent for histological analysis to ascertain the burn depth, after which the tissue was discarded. Tissues from 40 patients were estimated to be needed. For all patients (from patient/journal) the following was noted: age, gender, and body area that the skin comes from. For burns, the following was noted: damage date, injury time, type of burn (flame scalding, contact burn, etc., as shown in Figure 3.12d), tissue thickness (Figure 3.12e), and the physician's assessment of the burn depth.

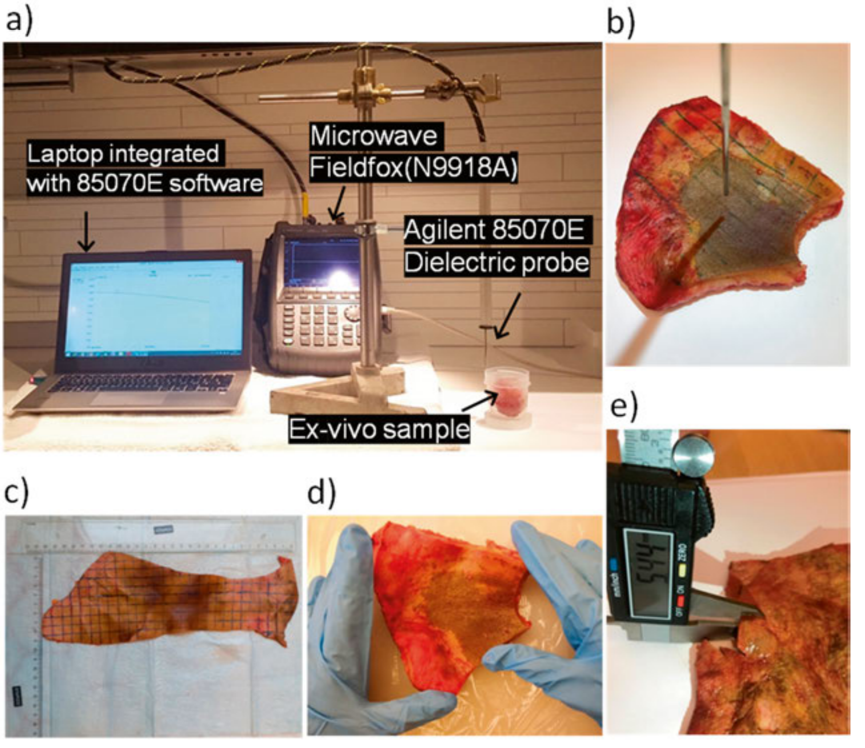

Figure 3.12 a) A photograph of the dielectric measurement setup of the ex-vivo burned tissue. b) Sample was measured using a dielectric probe. c) Samples were divided into homogeneous grid-sectors. d) Type of burn, damage date, and injury time were recorded for each sample. e) Metadata for the sample was recorded for further study.

4 Results and Discussion

In this section, the main results of **Paper I** to **Paper VI** are summarized. The use of a microwave sensor-based monitoring system during this thesis for laboratory and clinical examples to study its influence on microwave signals is presented. The described microwave sensors were fabricated through the process as described in Subsections 3.2.1 and 3.2.2, demonstrating the feasibility of the microwave sensor-based monitoring system in medical applications. In Subsection 3.4.4, dielectric permittivity characterization at microwave frequencies of ex-vivo human samples was carried out. This work is also currently being conducted as part of research and development.

4.1 New approach to microwave reflectivity and ultrasound measurements (Paper I)

In this study, a new approach was introduced to investigate the penetration depth evaluation of microwave sensors based on the split ring resonator in the in-vivo context of lower extremity areas. This approach is based on the optimization of a 3-D simulation model that used the CST Microwave Studio platform. The 3-D simulation model also consists of the sensor type mentioned in Subsection 3.1.2 and a multi-layered tissue representing the lower extremity, specifically in the femoral area. The geometry of the layered tissue is based on information acquired from ultrasound images (see Figures 4.1a–b) and primarily involved the thicknesses of muscle, skin, and fat. The different characteristics of the tissue layers and their appearances were documented with the help of a radiologist.

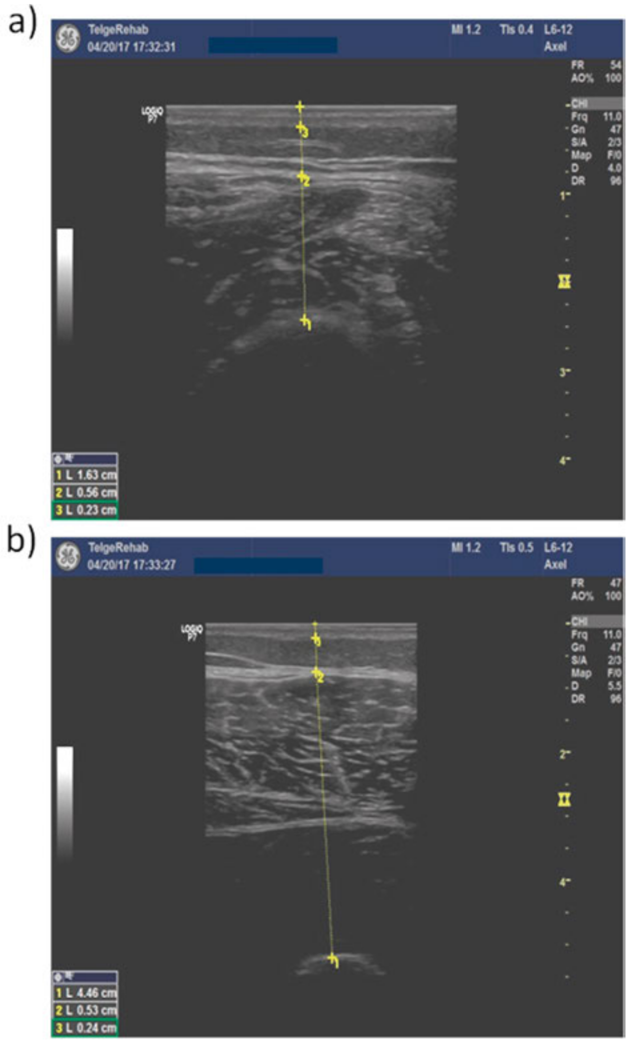

Figure 4.1 Measurement of tissue thickness of a volunteer performed using an ultrasound tool. a) Anterior of the distal femur 3 cm above the patella. b) Anterior of the thigh (10 cm above the patella) midlength. © 2018 Sensors. Reprinted, with permission, from [Mohd Shah, S.R., Velander, J., Mathur, P., et al. Split-ring resonator sensor penetration depth assessment using in vivo microwave reflectivity and ultrasound measurements for lower extremity trauma rehabilitation, Sensors, Feb. 2018].[94]

At Telge Rehabilitation Center, Södertälje, Sweden, data was collected during the Complex Fracture Orthopedic Rehabilitation (COMFORT) clinical assessment campaign from four volunteers who had given prior consent. The collection of information was executed under Swedish ethical approval (Appendix B). In the case of lower extremity injuries, the area around the femur bone is of particular interest.

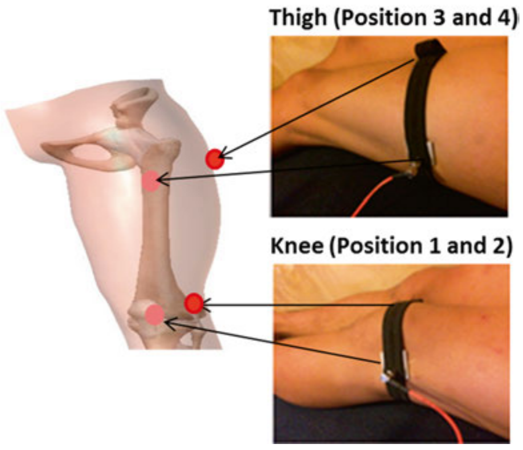

Figure 4.2 The proposed microwave sensor connected to the two positions of the distal femur and the thigh with a coaxial cable. . © 2018 Sensors. Reprinted, with permission, from [Mohd Shah, S.R., Velander, J., Mathur, P., et al. Split-ring resonator sensor penetration depth assessment using in vivo microwave reflectivity and ultrasound measurements for lower extremity trauma rehabilitation, Sensors, Feb. 2018].[94]

Figure 4.2 shows four different positions of the femoral area which were utilized for data collection:

Position 1: The distal femur anterior 3 cm above the patella.
Position 2: The distal femur lateral.
Position 3: The midlength of the anterior thigh 10 cm above the patella.
Position 4: The midlength of the lateral thigh.

The process of developing the 3-D simulation model until the stage of analyzing the penetration depth is shown in Figure 4.3. In this process, the optimization target for the sensor is the measured S_{11} parameters whereas the fitting parameters are the permittivity of each tissue layer. For this purpose, the values of effective permittivity of the tissues have to be studied by examining each position of the tissues with a simulated numerical model. The dielectric properties, in particular, consist of the relative permittivity and conductivity for which the numerical model has been trained. The S_{11} parameter measurements at various volunteer femoral positions were used as target data to train the proposed model in order to acquire effective permittivity for various volunteer tissues (muscle, fat, and skin). Compelling results were found in the muscle tissue layer, in which the layer possessed the highest dielectric properties and has the ability to detune the sensor resonance more than other tissue layers. It can be seen that for the variation of the effective permittivity, $\Delta\varepsilon_r$, the accuracy was within 0.38%, whereas the variation of the conductivity, $\Delta\sigma$, had an accuracy within 3.5%, compared to the literature data.

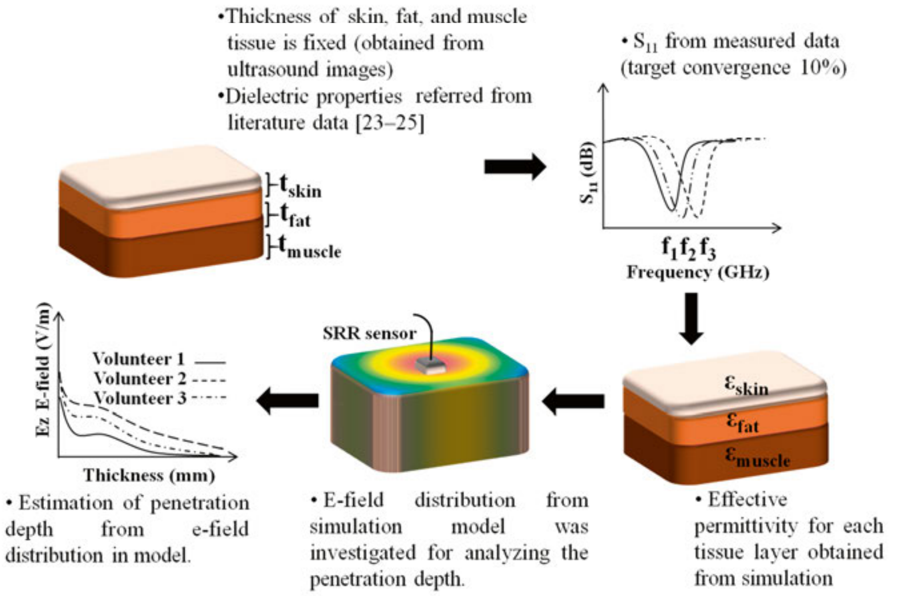

Figure 4.3 Process of extracting the dielectric profile of different tissues and the signal penetration depth using S_{11} data and ultrasound images. © 2018 Sensors. Reprinted, with permission, from [Mohd Shah, S.R., Velander, J., Mathur, P., et al. Split-ring resonator sensor penetration depth assessment using in vivo microwave reflectivity and ultrasound measurements for lower extremity trauma rehabilitation, Sensors, Feb. 2018].[94]

In order to study the dependence of the resonance frequency on the position of the femoral area, the S_{11} results from the clinical data measurements and their analyses are presented. Figures 4.4a–d illustrate the individual measurements for positions 1 to 4. A general trend showed that the tissue thickness and the position points influenced the sensor resonance frequency. The highest frequency shift was obtained at position 1 as shown in Figure 4.4a for volunteer 3 with a frequency shift of 30.1 MHz for calculations based on the shifted resonance frequency. The lowest calculated frequency shift was obtained at position 4 for volunteer 4 with a frequency shift of 17.1 MHz. It is evident from these results that the variation in tissue thickness at each position has a significant effect on the shift in the resonance frequency. With reference to the resonance frequency, f_r, the impact of the tissue's dielectric characteristics can also be noted for different measurement setups. The results demonstrate that when a thicker muscle tissue layer is present at the position involved, the resonance frequency may shift downwards from the sensor's free space resonance. When the muscle tissue layer is thinner, the resonance frequency may move upwards the sensor's free space resonance.

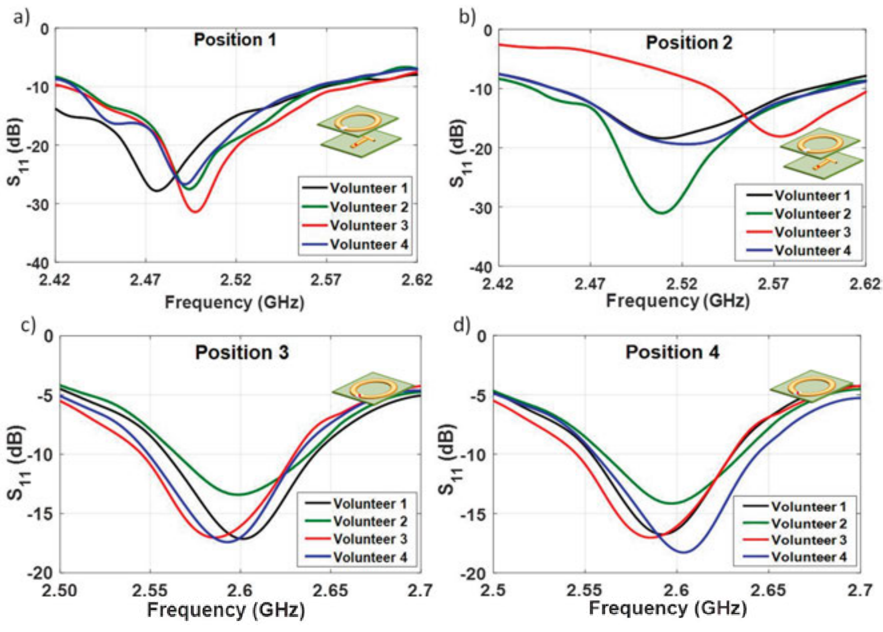

Figure 4.4 Measured S_{11} data versus frequency response for volunteers from different position measurements. a) Position 1: anterior of the distal femur. b) Position 2: lateral (outside) of the distal femur. c) Position 3: anterior of the thigh. d) Position 4: lateral of the thigh. © 2018 Sensors. Reprinted, with permission, from [Mohd Shah, S.R., Velander, J., Mathur, P., et al. Split-ring resonator sensor penetration depth assessment using in vivo microwave reflectivity and ultrasound measurements for lower extremity trauma rehabilitation, Sensors, Feb. 2018].[94]

The penetration depth was further analyzed by examining the E-field distribution in 3-D simulations of the optimized model for each of the considered positions. Figures 4.5a–d show the results of the E-field distribution with reference to the tissue thickness. The maximum value of the E-field distribution was considered as an indication point when the sensor was closely attached to the volunteer's body, i.e. when the distance was 0 mm. Thus, as the distance (with reference to the total thickness of the tissue) increased, the E-field penetration decreased gradually. In this case, the penetration depth attained was from 11.5 mm to 18 mm. According to the data on the tissue thickness acquired from the ultrasound measurements, the total E-field distribution from the skin to the muscle boundary covered a minimum of 46.3%.

Taking into account the tissue thickness data, when a thicker fat layer was present, the penetration depth was found to be larger. The thickness of the fat layer was thus observed to have a substantial effect on the E-field distribution. The penetration depth reduced gradually once the E-field distribution reached a mean fat thickness of 9.2 mm. This is because, due to its

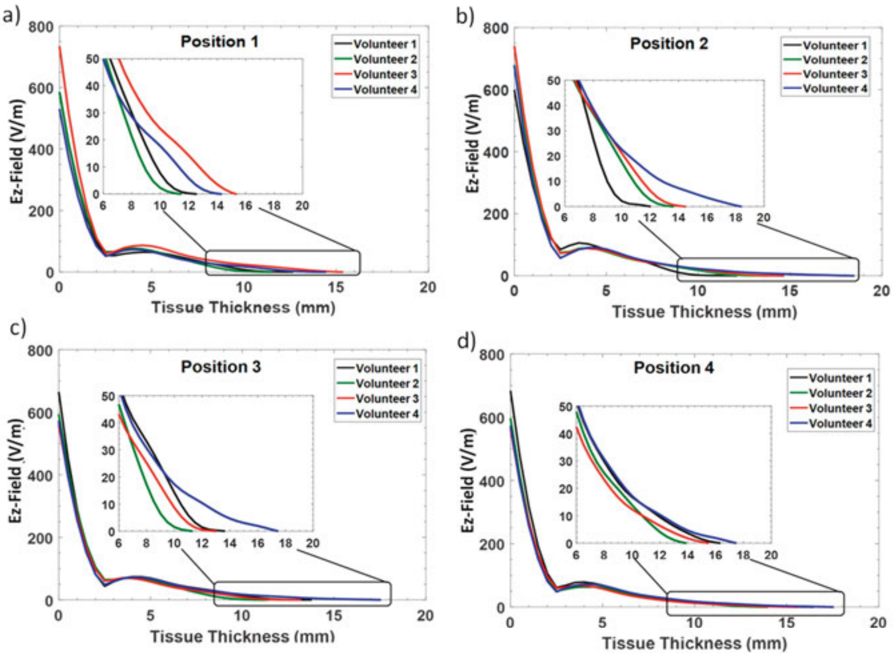

Figure 4.5 a)–d) Plot of the E-field penetration for different positions of tissue thicknesses. © 2018 Sensors. Reprinted, with permission, from [Mohd Shah, S.R., Velander, J., Mathur, P., et al. Split-ring resonator sensor penetration depth assessment using in vivo microwave reflectivity and ultrasound measurements for lower extremity trauma rehabilitation, Sensors, Feb. 2018].[94]

lower conductivity, the E-field penetrated more into the fat tissues. On the other hand, given that the tissue properties were a loss medium, the E-fields penetrated in the human body when the human body was exposed to the RF electromagnetic field.[108–110] As a result, the signal penetration depth for this measurement scenario depends on the tissue thickness which has lower conductivity such as the fat layer.

In addition, the correlation between the E-field and the distance can be clarified by using the energy propagation relationship and fat layer absorption. When the fat thickness increased, due to its lower loss compared to other tissue layers, the energy will be more easily transferred into fat. All of these conditions could be clarified by Asan et al., 2017, which is linked to the effect of the fat layer as a channel medium for intra-body communication.[111–112] Based on these findings, the signal transmission can be enhanced with the thickness of fat and muscle tissues. The signal transmission was evaluated in relation to the tissue channel's length and thickness.

Summary

A clinical measurement campaign was conducted with the involvement of 4 volunteers who had given prior consent, S_{11} measurements were performed, and tissue thickness information was acquired for the femoral area from ultrasound images. Numerical models were developed and individual tissue permittivity was acquired. The numerical model was utilized to simulate the E-field distribution after calculating the penetration depth. Resonance frequency was noted to be significantly influenced by a particular position of the measurement on the femoral area. The penetration depth at any specified place also depends on the tissue thickness which has lower conductivity such as the fat layer. This study showed that the proposed method can be used to estimate penetration depth by using information from the S_{11} sensor measurements and tissue thicknesses from ultrasound images. Therefore, preliminary results are encouraging and highlighted the effectiveness of using non-invasive methods to monitor tissue variations, especially during the rehabilitation of lower extremity fractures.

4.2 Study protocol of Complex Fracture Orthopedic Rehabilitation, COMFORT (Paper II)

Proximal femur fractures are a common injury ensuing low-energy trauma among the elderly. Most rehabilitation programs are based on restoring mobility and weight bearing recovery. However, compliance with therapy is quite low for patients with lower extremity fractures. Furthermore, the significance of gait parameters and how to manage rehabilitation after proximal femur fractures among the elderly are not firmly established. Therefore, the aim of this study protocol plays a major role in evaluating whether therapy compliance can be further improved with real-time visual biofeedback after proximal femur fractures among the elderly.

The study protocol can be fulfilled by selecting participants at random in either the control group receiving the usual treatment/care or the intervention group receiving real-time visual biofeedback on the weight bearing during the gait as well as the usual treatment/care. In addition to the normal institutional protocol, participants in the intervention group received real-time visual biofeedback on the weight bearing during a 30-meter walk using the SensiStep ambulatory biofeedback system (Evalan BV, Amsterdam, The Netherlands).

Consequently, this randomized controlled trial (RCT) will, therefore, provide real-time visual biofeedback to the patient and healthcare professionals within the clinical setting. The healthcare professionals are an international and multicenter trial that took place in the Netherlands and Sweden between March 2017 and August 2018 (Table 4.1).

Table 4.2. Healthcare professional clinics in the Netherlands (NL) and Sweden (SE).

Allocation (Group)	Rehabilitation clinics	Place
Control	Beweging 3.0 Meander Medical Center Maatweg 3 3813 TZ Amersfoort	Amersfoort (NL)
Control	Beweging 3.0 Woonzorgcentrum De Pol Vetkamp 85 3862 JN Nijkerk	Nijkerk (NL)
Control	Cordaan In het Zomerpark Remmersteinpark 3–5 2151 KE Nieuw-Vennep	Nieuw-Vennep (NL)
Control	azM Herstelzorg Sint Pieterstraat 23 6211 JM Maastricht	Maastricht (NL)
Control	Careyn Nieuw Tamarinde Neckardreef 6 3562 CN Utrecht	Utrecht (NL)
Control	Telge Rehab Östra Kanalgatan 2 152 71 Södertälje	Södertälje (SE)
Intervention	Zorgspectrum Geinsche Hof Vuurscheschans 75 3432 TX Nieuwegein	Nieuwegein (NL)
Intervention	Warande Bovenwegen Heideweg 2 3708 AT Zeist	Zeist (NL)
Intervention	Warande Diakonessenhuis Professor Lorentzlaan 76 3707 HL Zeist	Zeist (NL)
Intervention	Evean Schoenerstraat 11 1034 XZ Amsterdam	Amsterdam (NL)
Intervention	Zorggroep Groningen Schaaksport 100–102 9728 PG Groningen	Groningen (NL)

Before conducting the study, strict inclusion criteria were used to establish group homogeneity. The criteria for the inclusion of participants are that the participants are not older than 60 years, had a proximal femur fracture following low-energy trauma, had unrestricted weight bearing, had an expected clinical rehabilitation duration time of up to 2 weeks, and had a bodyweight below 120 kg. The criteria for the exclusion of participants include cognitive impairment and limited mobility before the trauma.

	STUDY PERIOD							
	Enrolment	Allocation	Post-allocation					Close-out
TIMEPOINT	*$-t_1$*	*t_0 (start)*	*t_1*	*t_2*	*t_3*	*t_4*	*etc.*	*t_x (end)*
ENROLMENT:								
Eligibility screen	X							
Informed consent	X							
MMSE	X							
Allocation		X						
INTERVENTIONS:								
SensiStep measurement without feedback *(Control group)*			←—	——	——	——	—→	
SensiStep measurement with feedback *(Intervention group)*			←—	——	——	——	—→	
ASSESSMENTS:								
EMS			←—	——	——	——	—→	
FAC			←—	——	——	——	—→	
VAS (pain)			←—	——	——	——	—→	
DOCUMENTATION:								
Note patient demographics		X						
Note date of discharge								X

Figure 4.6 Form of enrollment, documentation, assessments, and interventions. Elderly Mobility Scale (EMS), Functional Ambulation Categories (FAC), Mini-Mental State Examination (MMSE), Visual Analogue Scale (VAS). © 2018 Trials. Reprinted, with permission, from [Raaben, M., Mohd Shah, S.R., Augustine, R., Blokhuis, T. J. COMplex Fracture Orthopedic Rehabilitation (COMFORT) - Real-time visual biofeedback on weight bearing versus standard training methods in the treatment of proximal femur fractures in the elderly: study protocol for a multicenter randomized controlled trial, Trials, Apr. 2018].[113]

The clinical data was collected under the strict protocol, as shown in Figure 4.6. The site investigator asked participants who fulfilled the inclusion criteria to participate in the research and provided them with a letter of information with the study protocol and study purposes. Informed consent was signed and the cognitive score was assessed using Mini-Mental State Examination (MMSE).

Data was collected from the participants in accordance with the following trial protocol after informed consent and MMSE. Additional clinical trials were performed to gain further insight into each participant's rehabilitation progress; (i) Visual Analogue Scale (VAS) which was conducted daily, (ii) Functional Ambulation Categories (FAC) which was conducted once a week, and (iii) Elderly Mobility Scale (EMS) which was conducted twice a week. Finally, additional data for each participant was recorded such as age, gender, height, weight, date of surgery, type of surgery, walking aid, and length of admission to the rehabilitation center.

Summary

The study protocol for the multicenter randomized controlled trial was obtained by assessing whether real-time visual biofeedback on weight bearing versus conventional training techniques can enhance therapy compliance for the treatment of proximal femur fractures among the elderly. Consequently, the hypothesis that real-time biofeedback in weight bearing among the elderly after proximal femur fractures significantly improved. This improvement included the step duration and gait parameters maximum peak load, compared to the conventional training method. Second, improvements in gait parameters were hypothesized to have led to improvements in clinical scores, such as EMS, FAC, and VAS. This may result in enhanced rehabilitation (e.g. enhanced functional outcome), earlier rehabilitation, and reduced medical expenses.

4.3 Dielectric profiles at microwave frequencies of burn injuries

This works aims to find the functional relationship between the dielectric profiles and the burn depth of human burnt skin. We made two evaluation methods to analyze burnt skin. The first method is by measuring the permittivity characteristics and the second method is studying color variation using quantitative evaluation of 2-D dielectric image profiles.

4.3.1 Flexible microwave split ring resonator sensor (Paper III)

In order to examine different burn injuries by using a dielectric profile method, the development of the microwave SRR sensor onto flexible polydimethylsiloxane (PDMS) substrates is necessary.[99] As mentioned in the previous Subsection 3.2.2, PDMS is a promising flexible substrate material due to its water resistance, mechanical stability, inertness, and biocompatible characteristics.

In this study, a flexible sensor approach is presented to develop a portable, low cost, safe, and non-invasive microwave sensor-based diagnostic tool for the analysis of burns. The tool will facilitate an early diagnosis, and monitor and treat burn patients by providing reliable and accurate diagnosis data concerning burn area and burn depth. The tool can diagnose the actual burn area and burn depth accurately and successfully and enable early medical intervention of the burn injuries.

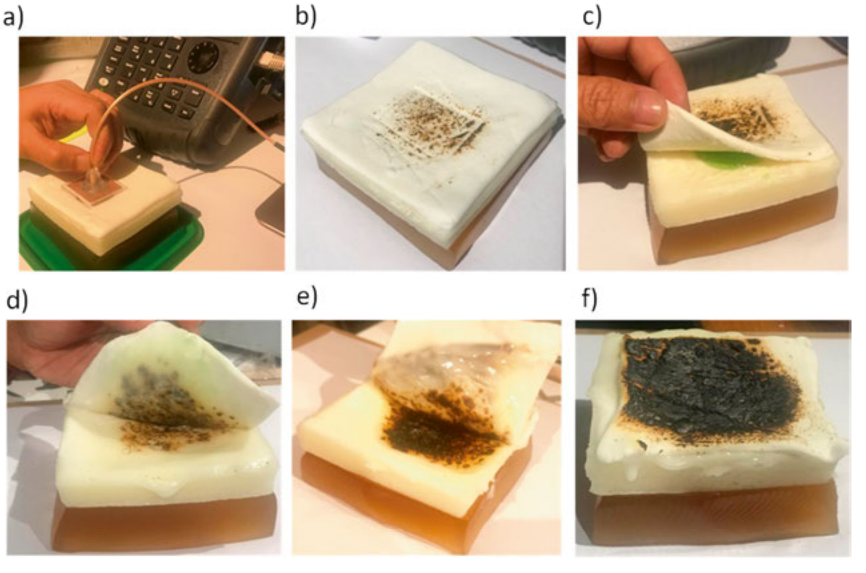

Figure 4.7 The proposed sensor position with different conditions of burn injuries. a) Normal condition. b) Stage 1. c) Stage 2 by implementing blistering condition. d) Stage 3. e) Stage 4 in which skin is dry and leathery. f) Stage 5 full-thickness burn. © 2019 IEEE. Reprinted, with permission, from [Mohd Shah, S.R., Velander, J., Perez, M.D., et al. Improved sensor for non-invasive assessment of burn injury depth using microwave reflectometry, 13th European Conference on Antennas and Propagation (EuCAP), Krakow, Poland, Mar. 2019].[99]

The non-invasive diagnostic tool and the fabrication process of the sensor are the main developments regarding its precedent microwave sensor based on the PDMS and copper materials. In order to validate the conceptual functionality of the proposed sensor, human tissue emulating phantoms were designed, fabricated, verified, and employed to emulate different burn depths as shown in Figures 4.7a–f.

The following was performed on different parts of the phantoms to imitate the different stages of burn depth:

i. An adjustable refillable blowtorch flame was used to burn the phantom on the surfaces of the various phantom components to decrease their water content and generate combustion (Figures 4.7b–f)
ii. Water pockets were included to emulate inflammation using gels with high water content (Figure 4.7c)

The various phantom stages representing the different burning stages were thus modeled and described as follows:

1. Normal condition: Figure 4.7a shows that the three homogeneous layers of skin, fat and muscle tissue are intact.
2. Stage 1: The superficial burn is represented by a minor burn on the skin surface as shown in Figure 4.7b.
3. Stage 2: The superficial partial-thickness burn is represented by adding the blistering condition with an accumulation of water pockets between the skin and the fat layers as shown in Figure 4.7c.
4. Stage 3: The deep dermal partial-thickness burn is represented by the skin on both sides which are burned and partially burned on the top side of the fat layer as shown in Figure 4.7d.
5. Stage 4: The full-thickness burn is represented by the skin which was treated much more on both sides which are dry and leathery as shown in Figure 4.7e.
6. Stage 5: The full-thickness burn is represented by subcutaneous fatty tissue, sometimes bones, muscles, joints, and tendons are damaged (Figure 4.7f).

The differences in resonance frequency for various dielectric constants with regard to phantom layers are shown in Figure 4.8. By measuring the reflection coefficient, an inverse linear correlation was found between the measured resonance frequency and dielectric permittivity of each phantom layer.

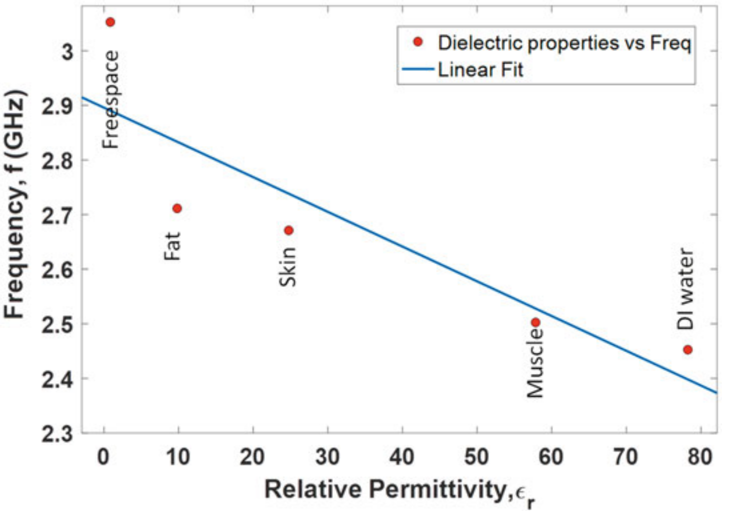

Figure 4.8 The resonance frequency measurement of the sensor with respect to changes in the dielectric properties of each phantom layer. from [Mohd Shah, S.R., Velander, J., Perez, M.D., et al. Improved sensor for non-invasive assessment of burn injury depth using microwave reflectometry, 13th European Conference on Antennas and Propagation (EuCAP), Krakow, Poland, Mar. 2019].[99]

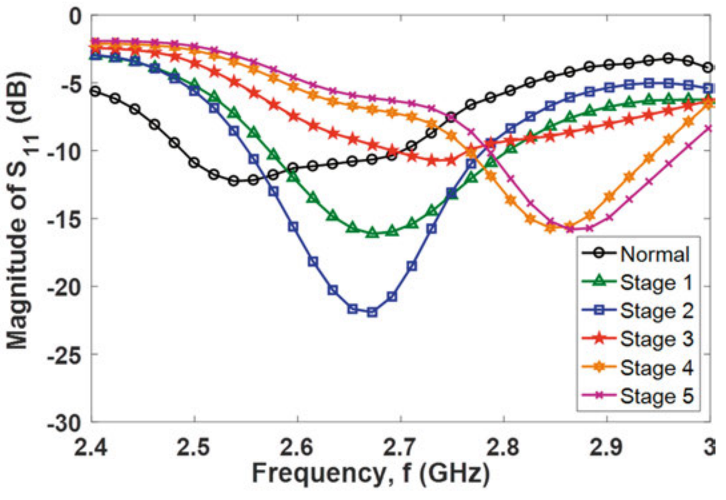

Figure 4.9 Measured S_{11} at different resonance frequencies and different burning stages with regard to the normal condition. from [Mohd Shah, S.R., Velander, J., Perez, M.D., et al. Improved sensor for non-invasive assessment of burn injury depth using microwave reflectometry, 13th European Conference on Antennas and Propagation (EuCAP), Krakow, Poland, Mar. 2019].[99]

Figure 4.9 shows the results of the magnitude of the reflection coefficient, S_{11} with respect to the different phantoms' burn stages. As shown in Figure 4.9, there are discrepancies between the normal condition and Stages 1 and 2, and between Stage 3 and Stages 4 and 5.

The sensor performed sensibly well for all the burn injuries. Results indicated that the sensor could accurately sense the accumulation of water pockets on the Stage 2 burn injury with a magnitude difference of about 10 dB and a shift frequency difference of 170 MHz between normal conditions. This shows that this Stage 2 burn contributed to the highest magnitude compared to the normal skin, which is evident from inflammation/edema under the skin layer due to higher water proportion.

In addition, the accuracy of the sensor was observed in Stage 5 with a magnitude difference of approximately 8 dB and a frequency shift of 345 MHz obtained for leathery skin. The results indicated that the decrease in the tissue water content and the decrease in the phantom's water holding capacity over the dehydration period led to an increase in the drip-loss and thus influenced the measurement of shifted resonance.

Summary

The ability of the flexible microwave sensor to assess burn injury depth was presented in **Paper III**. These preliminary results suggested proof-of-concept: it is possible to distinguish different burn depths by their respective dielectric profiles. To support this work, a database with a dielectric constant list of different burn injury conditions is needed. By looking at the respective dielectric profile, this will eventually provide a comprehensive understanding of different burn depths. From this analysis, measuring ex-vivo burned skin removed from burn patients during routine surgery will evaluate the performance of this flexible microwave sensor.

4.3.2 Assessment of burn depth on burnt skin samples

In order to understand the stage of burn injuries related to the dielectric profile at microwave frequencies of different burning depths, preliminary data from ex-vivo human (burnt) skin samples are presented. In the SenseBurn project, the MMG received different burn samples from the Burn Center at Uppsala University Hospital. The tissue was placed in a sterile jar and placed in a refrigerator while waiting for it to be transported to the Ångström Laboratory, Uppsala University. Currently, as part of research and development, dielectric spectroscopic characterization at microwave frequencies of ex-vivo human samples is being carried out. First, a picture of the sample was taken and saved as shown in Figure 4.10a. The collected data was then encrypted and stored on a secure server and is accessible by the doctor to evaluate the burn depth.

Hence, every received burn-injured sample was sectorized (divided into sectors) as shown in Figure 4.10b. Every sector represents a unit, a sample in which every sector/unit has four estimates: normalized dielectric permittivity at 2.45 GHz (Figure 4.10c), normalized loss tangent, normalized color, and predominant clinical opinions agreement. The normalized dielectric permittivity and loss tangent estimates need to be the best estimates for every sector.

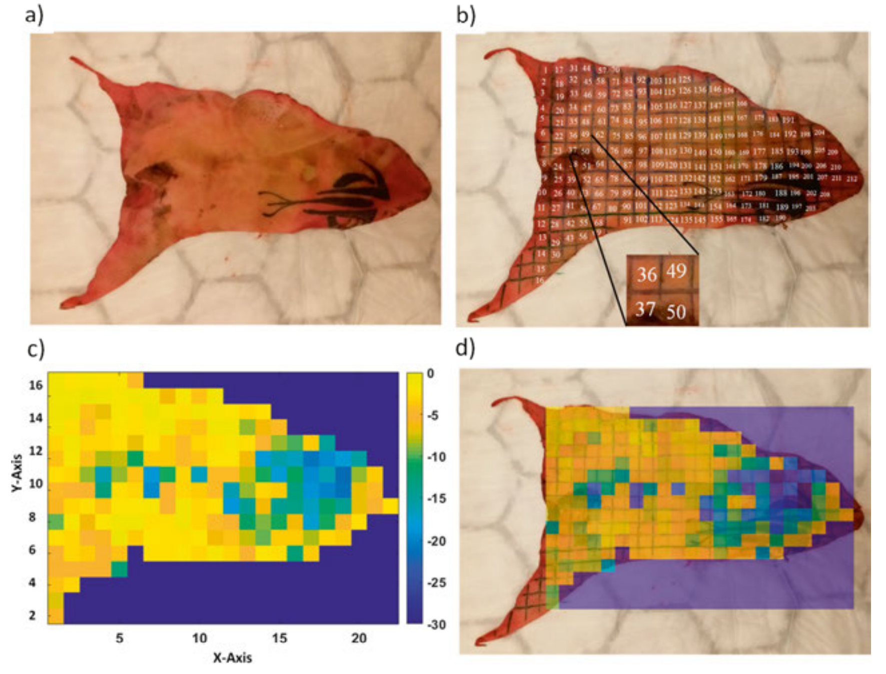

Figure 4.10 Photograph of ex-vivo measurement on burn injury sample. a) Photograph of burnt skin sample from a patient who had undergone a surgical operation of an acute burn. b) Sample sectorized into different sectors. c) Normalized dielectric permittivity at frequency 2.45 GHz. d) 2-D image shows the permittivity (for each sector) as colors on top of the sample image.

A 2-D image (Figure 4.10d) based on the permittivity characteristic of the sample is presented. The concept is similar to microwave imaging and in correlation with dielectric properties whereby distinguishing between healthy and burned skin can be achieved. In order to classify the degree of the burnt sample, it was necessary to define a threshold for each degree of the burn. The most reliable definition of the degree of the burn can be provided by the burn surgical experts. In the ensuing lines, the protocol for the measurement was provided, which was described in detail in Subsection 3.5.2.

Summary

These preliminary results show a positive suggestion to proof-of-concept by which it is possible to distinguish different burn depths by their respective dielectric profiles. However, more information needs to be gathered to improve the accuracy of these results statistically. The proof-of-concept will make it possible to conduct an early diagnosis, and monitor and treat burn patients by providing reliable and precise diagnosis data concerning burn area and burn depth. The tool will help in diagnosing the actual burn area and burn depth accurately and successfully and enable early medical intervention of the burn injuries.

4.4 Clinical measurement of pediatric craniosynostosis patients (Paper IV)

In order to get proper monitoring of the bone healing progress in newborn children treated for craniosynostosis, it is very important to ensure good recovery of the cranial vault and assist to reduce trauma in the patient. Craniosynostosis is a medical condition defined as the premature fusion of one or more of the cranial sutures (skull plates) of a child's cranium.[114] In the cranial vault of newborns, lack of information on how bone mineralization progresses over time makes it challenging to quantitatively evaluate recovery after surgery. In order to decrease this gap, available techniques are significantly risky (e.g. X-ray and CT scan) for children and new solutions are being studied.

Microwave sensors operating at low microwave frequencies have been introduced in this thesis and could be used after surgical interventions to read some modifications in the structure of the superficial layers of the skull. This proposed solution as a diagnostic tool is being intensively studied in a pilot clinical campaign carried out in the BDAS project at the Ångström Laboratory and Akademiska Medical University Hospital, Uppsala, Sweden.[95, 104–107, 115] The project consortium comprises academic and industrial partners that are complementary in their expertise and contributions to the project.

The ability of an embedded system for the BDA tool was determined by numerical simulation, phantom mimicking, and clinical trials from a patient who had undergone craniosynostosis. The simulation analysis was performed using Computer Simulation Technology (CST Studio, 2018, SIMULIA, Dassault Systèmes, France). Resonance variability was first studied using a bone healing progression 3-D model that accounted for three layers (skin, skull, and brain) and where the thickness of the bone layer varied. Furthermore, it was also studied how sensor movements could affect output such as the condition of rotation, lift, shift, and tilt as shown in Figures 4.11a–e.

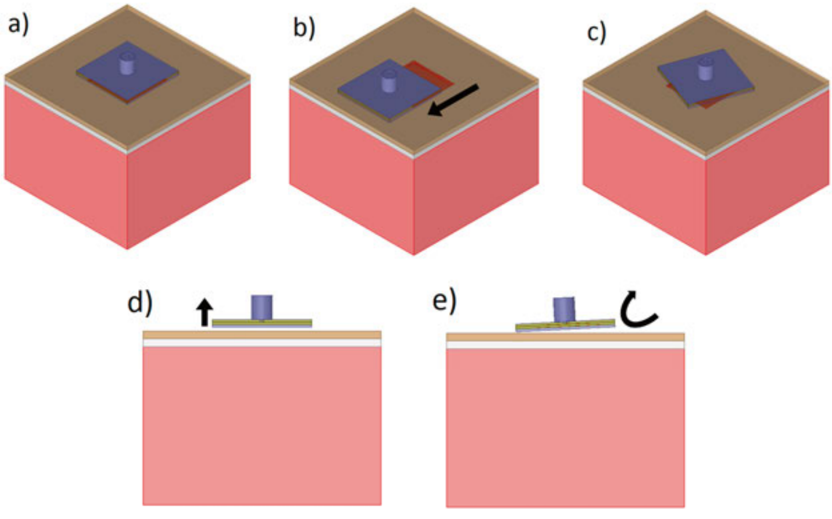

Figure 4.11 Simulation of microwave sensor on 3-D models. a) Reference position. b) 10 mm transition. c) 30º rotation. d) 1 mm lift above head phantom. e) 3º tilt.

To achieve the functionality of the sensor, laboratory trials were performed using Anthropomorphic Tissue Emulating (ATE) phantoms after the numerical analysis. The phantom section consisted of skin, skull, and brain tissues and was designed from the point of view of electromagnetic response. Different materials were used in the craniotomy phantoms fabrication process such as sodium chloride, gelatin, agar, calcium sulfate, polyethylene powder (PEP) of 25 µm particle size, deionized (DI) water, TX-151, and gypsum.[102] These materials are cost-effective, non-toxic, and easy to use. Phantom fabrication showed excellent outcomes for relative permittivity, ε_r, and loss tangent (δ) similar to real human tissues by choosing the right proportion of each material (see supplementary file in **Paper IV**).

The next step was performing the clinical trial using the microwave sensor and embedded system for BDA. This measurement campaign included 23 patients who had undergone surgery for non-syndromic craniosynostosis at Akademiska Medical University Hospital, Uppsala, Sweden. The patients were measured with the BDA sensor on a chosen reference position and 1–3 defect positions as shown in Figure 4.12.

Patients were measured at seven occasions: M1, preoperative; M2, postoperative; M3, 1 week after surgery; M4, 1 month after surgery; M5, 3 months after surgery; M6, 6 months after surgery; and M7, 1 year after surgery. Every measurement was analyzed by obtaining each parameter on the resonance frequency, f_{res} (GHz), the amplitude at the resonance frequency, A_{res} (dB), and the Q-factor at 3 dB, Q_3.[95, 104]

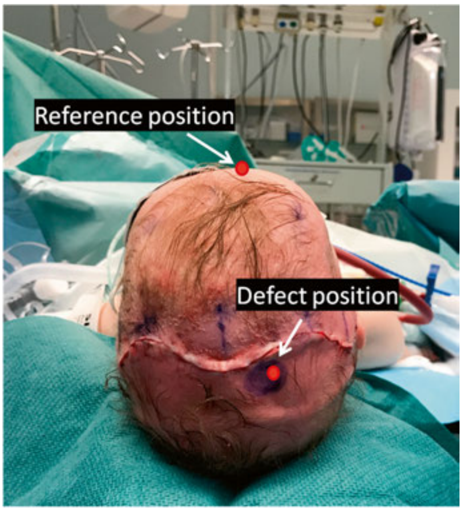

Figure 4.12 Location of measurement points on a chosen reference and possible defect locations on a newborn head post-surgery.

The analysis consisted of calculating the mean and standard deviation for all the points belonging to the same timepoint after extracting all the parameters for each dataset. Figures 4.13a–b show the analysis of the reference and defect points across the timepoints, where every timepoint has a different color. The results of the reference point indicated that all timepoints were consistent with $Q_3 \leq 10$ as shown in Figure 4.13a. This was expected because the reference measurements were performed at the same spot on the forehead.

Reference measurements were always performed on solid bone in contrast to the defect points that undergo different stages of the ossification process. In addition, the presence of muscle and thicker bone in the reference place influenced the outcome of the decreased Q-factor. These findings led us to suspect that the thicker muscle and skull bone lowered the resonance frequency and Q-factor (for all timepoints M1 to M7).

The clinical data was further analyzed on the skull defect to see the effects of the Q-factor on the healing progression. In Figure 4.13b, it can be observed that there is a significant difference in Q-factor between M1 and M2. This result made it evident that M1 was before the surgery when there was solid bone and M2 was after the surgery where there was a bone defect. The presence of blood and thinner skull on the defect point influenced the higher Q-factor and detuned the frequency shift due to the impact of inflammation or edema immediately after surgery. This edema may have affected the measurement as excess fluid can affect the resonance frequency at a lower level because of its water-based properties.

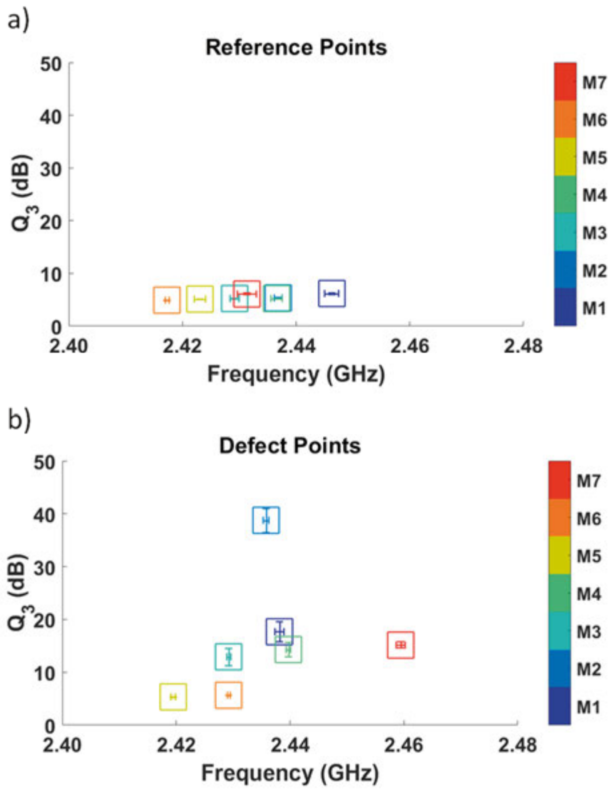

Figure 4.13 Mean and confidence interval for a) reference point. b) defect point. © 2019 Sensors. Reprinted, with permission, from [Mohd Shah, S. R., et al. Microwave-sensor-based clinical measurements for monitoring post-craniotomy bone development in pediatric craniosynostosis patients, Sensors, Sept. 2019].[95]

Summary

The embedded system for the BDA tool was demonstrated in this study together with the clinical campaign to analyze the variation of healing progression on craniosynostosis. In summary, we can conclude that the proposed BDA tool made it an easy tool to handle instruments that could offer direct visualization of changes associated with different bone healing stages without risking the health of the child with ionizing radiation. The study indicated, for the current configuration, that the system is more likely to identify tissue variations at an earlier stage (postoperative) than at later phases (1 year after surgery). In the data analysis, two hypotheses were developed and tested concerning the place of the measuring points with regard to the positioning and healing over time. By deriving a set of parameters for each gathered data set in the clinical studies, a distinctive pattern was discovered showing noticeable improvements with this method during the healing phase.

4.5 Two-port non-invasive microwave sensor (Paper V)

The goal of this work is to use a two-port non-invasive microwave sensor as an additional design parameter that in turn can be optimized to analyze the variations in biological tissue thickness.[116] The variations also take into account the effects of physiological and biological properties on microwave signals. From a clinical point of view, the variations in biological tissue thickness somehow can be referred to several medical conditions such as muscular atrophy, sarcopenia, etc. In secondary care such as geriatric and home care, the quality of life of the elderly is hampered by a decrease in muscle mass, an increased risk of falling, enhanced disease morbidity, and lower life expectancy.

DEXA, ultrasound scans, bioimpedance and measures of skeletal muscle mass are all used in terms of diagnsotic createria for sacropenia. Nevertheless, none of these methods show high precision or reproducibility, resulting in sarcopenia or muscular atrophy being underdiagnosed and there are still many challenges that need to be addressed. If diagnosed correctly, sarcopenia can be mitigated by exercise regimes and proper dietary supplements. While these interventions are cost-effective, the condition must be diagnosed before any treatment can be initiated and optimized continuously based on the composition and medical history of the patient.

In this study, the two-port method from the developed microwave sensor in Subsection 3.2.1 is presented to gain an understanding of how to solve these challenges. This method for tissue analysis is non-invasive, non-ionizing, and more practical compared to other state-of-the-art modalities. To validate the approach, the variability between different tissue thicknesses was used as a precursor to estimate the attenuation level of the signal, which in turn, is an indication of underlying tissue distribution. Finally, validation was performed between the electrical field (E-field) and the penetration depth and their related impacts on signal loss.

For the experiment setup, fresh porcine belly was used to emulate human tissue properties. These characteristics of the EM tissue are similar to those of human tissues.[82–83] Therefore, this tissue material provides an optimal environment for emulating human tissue. The three-layered tissue structure containing skin, fat, and muscle (top to bottom) was placed and arranged in a custom-made 3-D printed plastic case supported by a 5 mm thick plate below the muscle layer. A photograph of this experimental configuration is shown in Figures 4.14a–b. From this setup, the thickness of the skin layer (2.5 mm) stayed fixed to validate the impact of variation in fat and muscle layer. Meanwhile, the variation of fat thickness was adjusted from 5 mm to 35 mm in 10 mm steps and the muscle thickness was adjusted from 10 mm to 50 mm in 20 mm steps.

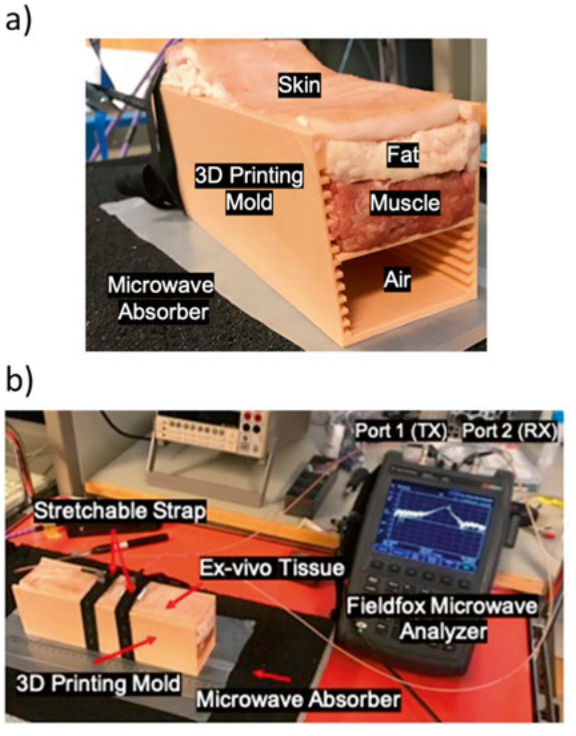

Figure 4.14 Photograph of the ex-vivo experimental setup. a) Multilayer homogeneous model of porcine tissue. b) Two-port microwave sensors connected to the Fieldfox Microwave Analyzer (N9918A). © 2019 IEEE. Reprinted, with permission, from [Mohd Shah, S.R., Asan, N.B., Velander, J., et al. Analysis of thickness variation in biological tissues using microwave sensors for health monitoring applications, IEEE Access, Sept. 2019].[116]

During the measurement, the distance between microwave sensors varied from 0 mm to 250 mm in 50 mm steps. An interesting result was observed where the fat thickness variations showed a very distinctive curve/pattern that can be used to differentiate the underlying tissue thickness as shown in Figures 4.15a–d. The results of this investigation provide a better understanding of the signal loss and can be used to estimate tissue thickness using a fixed position of the sensor. In order to inspect the E-field distribution and penetration depth between the microwave sensors, three experimental scenarios were considered:

- Scenario 1: Minimum thickness of the fat layer of 5 mm represents a thinner condition.
- Scenario 2: An average thickness of the fat layer of 25 mm represents a normal condition.
- Scenario 3: Maximum thickness of fat the layer of 35 mm represents a high-fat condition.

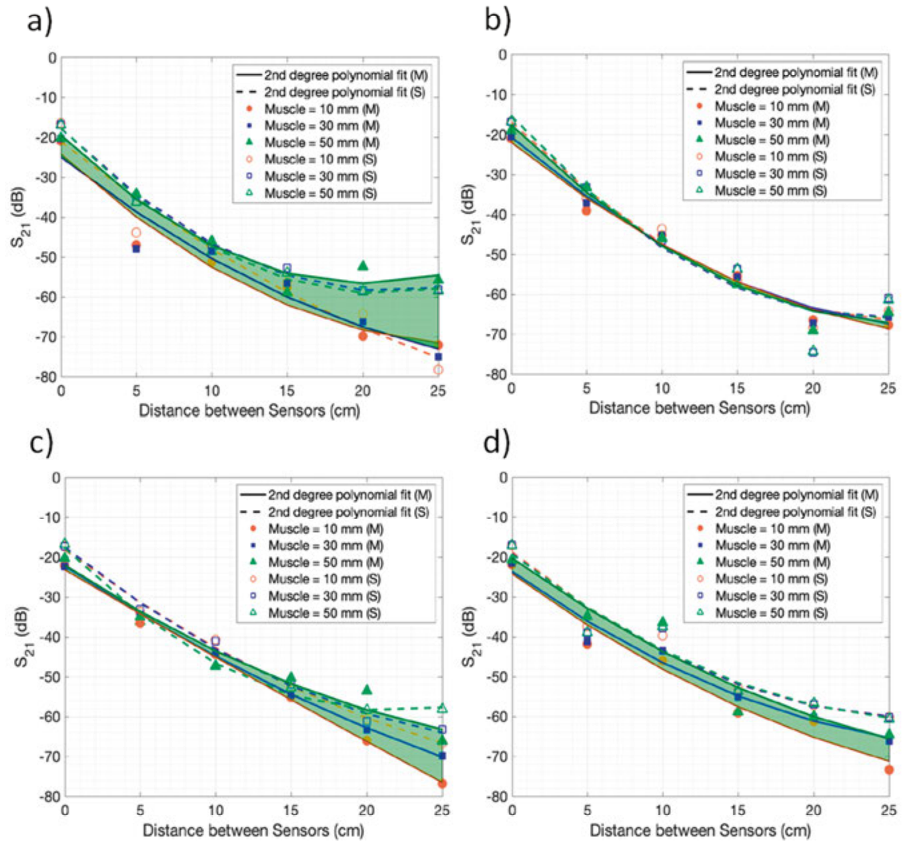

Figure 4.15 Simulated (– – line) and measured (– line) results with the distance variation of microwave sensors from 0 to 250 mm. © 2019 IEEE. Reprinted, with permission, from [Mohd Shah, S.R., Asan, N.B., Velander, J., et al. Analysis of thickness variation in biological tissues using microwave sensors for health monitoring applications, IEEE Access, Sept. 2019].[116]

Figure 4.16a describes the E-field distribution of the thinner condition in fat tissues, resulting in greater surface coupling and signal leakage. The E-field leaked from the fat layer to the surrounding free space outside of the skin layer. In this case, multiple reflections can be taken into account between the surface layer and the boundaries of the fat tissue. Figures 4.16b–c show that the increase of the fat layer allowed the E-field to further propagate through the muscle tissues. The signal for thicker fat was constantly attenuated as the outcomes are very comparable for scenarios 2 and 3. It is important to note that two important factors have been observed; i) absorption loss due to the dielectric properties of the material and ii) fewer reflection signals as it propagated across multiple layers of tissue.

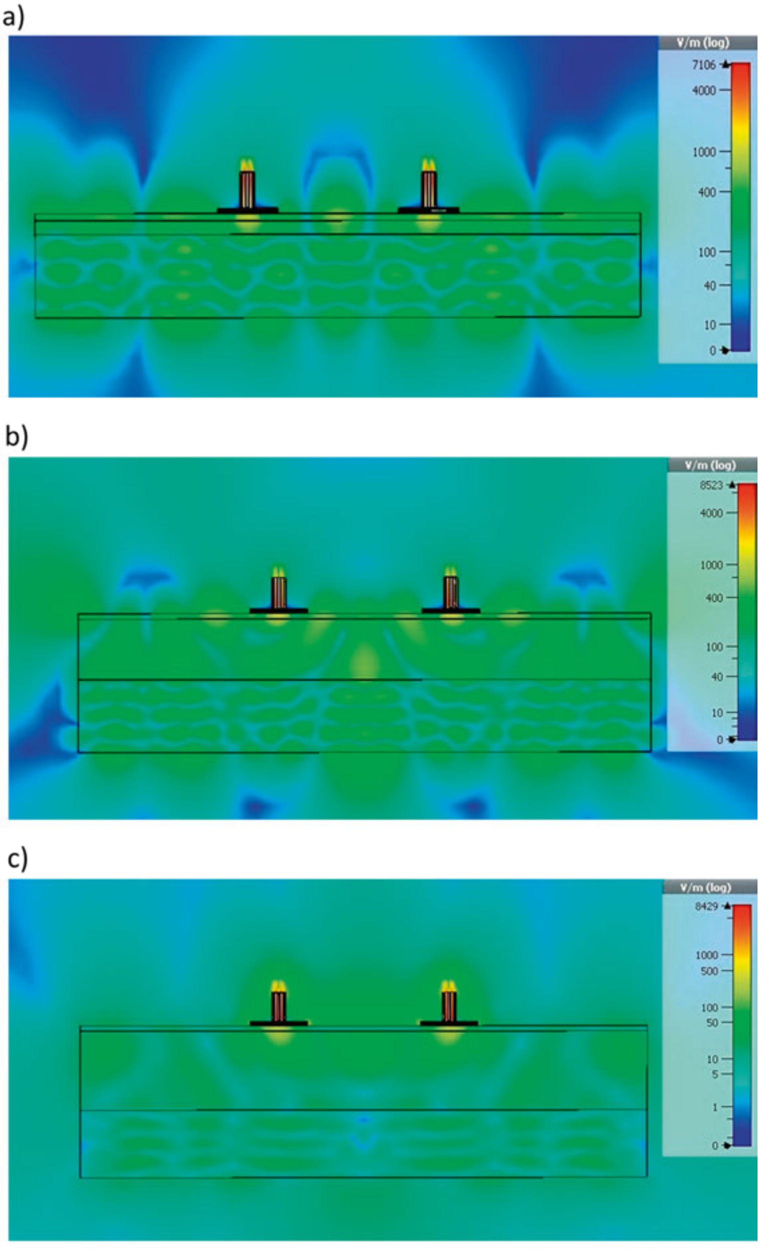

Figure 4.16 The E-field distribution on the tissue thickness of a) Fat = 5 mm. b) Fat = 25 mm. c) Fat = 35 mm. The distance between the SRR sensors was 100 mm for all the cases. © 2019 IEEE. Reprinted, with permission, from [Mohd Shah, S.R., Asan, N.B., Velander, J., et al. Analysis of thickness variation in biological tissues using microwave sensors for health monitoring applications, IEEE Access, Sept. 2019].[116]

Summary

New methods of investigating variations in tissue thickness while taking into account the physiological and biological effects on the microwave signals are presented. This approach is based on the two-port non-invasive microwave sensors and the experiment was performed by using a three-layer ex-vivo model. The attenuation of the EM signal was analyzed according to the tissue thickness and distance variations. Some mechanisms were addressed that influenced the signal paths through the ex-vivo tissues in terms of the E-field distribution and penetration depth.

1. The observation demonstrated that the attenuation of the EM signal through thicker fat has a higher signal loss on the ex-vivo model since it has lower conductivity.
2. There were significant differences in terms of the distance between the microwave sensors and the distribution of the E-field.

In addition, the impact of highly contrasting dielectric properties between the muscle and the fat layers strongly increased the depth of the penetration.

5. Conclusion and Recommendations

New concepts of medical diagnosis using the microwave technique were developed in this thesis, where the designs of the sensors are primarily used for microwave sensing and the dielectric imaging profile. The techniques pave way for the potential of new microwave medical diagnosis to be envisioned for a telemedicine healthcare system, where patients can be monitored in real time for medical advice. It is, therefore, possible to improve their mobility as well as their quality of care.

In this thesis, the concepts of resonator probe methods were evaluated in terms of both numerical analysis and experiments. In addition, the experiments were conducted in the laboratory at Uppsala University including the academic university hospital and the rehabilitation center in Sweden and in the Netherlands for data collection in clinical campaigns.

In this experimental work, the first part of the thesis analyzed different permittivity and thicknesses of human tissues. The propagation behavior of electromagnetic waves in human tissues was analyzed from the system point of view via quantitative investigation of human tissues with regard to their dielectric properties. Tissues with high water content such as blood and muscles exhibited low penetration depth, high relative permittivity, and high signal attenuation. On the other hand, tissues with low water content (e.g. skull and fat) showed low signal attenuation of electromagnetic waves. Furthermore, the results demonstrated that strong reflections occurred at the boundary between higher and lower water content tissues due to the presence of high dielectric contrast.

The second part of the thesis covered the clinical study from the perspectives of various medical conditions. Extensive works have been done to analyze the importance of a mechanism associated with bone healing. Such changes in the healing patterns were exhibited in both targeted areas (lower extremity trauma and craniosynostosis) and can typically detect changes over time. The results also showed that the microwave technique offers direct visualization of changes associated with different bone healing stages without risking the health of children or elderly people (both of which are the main groups of subjects in this thesis) by exposing them to ionizing radiation.

The final part of this thesis highlighted the possibility of examining different permittivity changes in skin burn tissue samples using the microwave sensing technique. The analysis of the tissue samples is combined with that of the artificial emulating phantoms via the open-ended and resonant probe methods. The aim is to improve our understanding of the samples and to further evolve the probes for other applications. As a result, microwave imaging which correlates with dielectric properties can make it possible to distinguish between healthy and affected samples. In general, the applicability of the microwave system with microwave-based sensors has been proven to be useful and can be utilized to diagnose medical conditions in the near future. Furthermore, the microwave technique is beneficial as it uses non-ionizing radiation which consequently enables in-vivo imaging to be done in a safe manner.

Future recommendations

In order to achieve the aforementioned goal, fundamental steps need to be taken, as outlined below:

1. Currently, the main part of the microwave medical system has been developed with the microwave sensor and control system, and tested it numerically and experimentally (in labs and hospitals). However, the results from the clinical study need to be compared with preoperative CT scans and an additional two-year or three-year follow-up is necessary.
2. More subjects (patients) need to be included to provide more material to compare the clinical measurements with the CT scans. This can be conducted effectively by using a newly developed program in the clinic that calculates a patient's healing progression from the information provided by CT scans.
3. In our future studies, additional parameters, such as phase, polarization, and impedance, can be added.
4. An enhanced multilayer model for effective permittivity would be beneficial for calculating and analyzing the data step-by-step from different perspectives. In addition, by minimizing the frequency spectrum, data will also be easier to process and make the time from measurement to analysis shorter.
5. The final interface of microwave sensing and imaging can be further integrated with the machine learning process to improve its clinical measurements and eventually be used for medical diagnosis.

6. Sammanfattning och perspektiv på svenska

Nya koncept där mikrovågsteknik för medicinär diagnos utvecklas i denna avhandling. Med denna teknik har sensor designats avsedda att mäta i mikrovågsbandet och för dielektrisk avbildning för biomedicinska tillämpningar. Denna teknik öppnar möjligheten för nya medicinska instrument som grundar sig i mikrovågsteknik som kan användas i en mer portabel vård. Så med denna teknik kan vården bli bättre och även mer portabel.

Också i denna avhandling så undersöks resonator metoder både genom numerisk analys men även genom experiment. Experimenten utfördes i labb på Uppsala Universitet. På Uppsala Akademiska sjukhus och kliniker i Sverige och Nederländerna har insamling av data skett genom mätkampanjer.

I det experimentella arbetet, den första delen av avhandlingen så analyseras permittiviteten och tjockleken för olika mänskliga vävnader. Propageringen av elektromagnetiska vågor i mänskliga vävnader analyserades från ett kvantitativt perspektiv. Vävnader med en hög andel vatten såsom muskler och blod påvisade låg penetrationsdjup av signalen, hög permittivitet och hög försvagnining av signalen. Å andra sidan så visade vävnader med låg andel vatten (till exempel ben och fett) på låg försvagning av den elektromagnetiska signalen. Utöver det så visade resultaten även på starka reflektioner skedde vid gränsen mellan vävnader med hög och låg vattenhalt på grund av den starka dielektriska kontrasten.

Andra delen av avhandlingen berör de kliniska studierna som utförts på olika medicinska tillstånd. Mycket arbete har lagts på att hitta en metod för att undersöka och diagnostisera läkningen av skelett vid frakturer. För skelettdefekter så påvisades ett mönster i läkningsprocessen för båda typen av defekter som undersöktes, kraniosynostos och benbrott. Resultatet av detta är att vi med hjälp av mikrovågstekniken kan erbjuda en visualisering av läkningsprocessen utan att riskera hälsan hos barn och äldre personer, som var målgrupperna för dessa projekt, genom att utsätta de för röntgenstrålning.

I sista delen av denna avhandling så undersöks möjligheten av att mäta skillnaden i permittivitet på brännskadad hud jämfört med icke-brännskadad hud genom att använda samma mikrovågssensorer. Analysen av proven på brännskadad hud kombineras med artificiella material som tillverkas för att efterlikna mänsklig hud så de delar hudens dielektriska egenskaper. Dessa prov undersöks både med koaxial prob med öppna ändar och resonator prob. Anledningen till detta är att öka vår förståelse av proven och även förståelsen av proberna för andra applikationer. Resultatet av detta visar att vi med hjälp av sensorerna kan upptäcka en skillnad mellan skadadade och friska prov.

För att summera kan det sägas att microvågssystem med sensorer baserade på mikrovågsteknik har visat sig användbara och kan användas för att diagnostisera medicinska tillstånd i en nära framtid. Dessutom har mikrovågsteknik förde jämfört med andra metoder då patienten inte behöver utsättas för röntgenstrålning och in-vivo avbildining kan göras på ett säkrare sätt.

Framtida rekommendationer

För att kunna nå det nämnda målet behöver, nedan listade steg tas:

1. Hittills har det utvecklade medicinska mikrovågssystemet, bestående av sensor och kontrollenhet, testas numeriskt och experimentellt (i laboratorier och på sjukhus). Men dessa mätresultat behöver jämföras med datortomografi-undersökningar som gjorts före operationen och uppföljningar mäste göras upp till två eller tre år efter operationen.
2. Flera patienter mäste delta i undersökningarna så att jämföreksen mellan de kliniska mikrovågsmätningrana och datortomografiundersökningarna blir mer pålitliga. Detta kan enkelt göras genom ett nyutvecklat program som finns tillgängligt på klinikerna som beräknar patientens läkningsframsteg från information från datortomografi.
3. Analysen kan utöka genom att inkludera flera parametrar såsom fas, polarisering och impedans.
4. En förbättrad multi-lager modell för att beräkna effektiv permittivitet i material bestående av flera olika lager behövs för att beräkna och analysera datan steg för steg från olika perspektiv. Dessutom skulle en minskning av frekvensområdet göra datat enklare att processa och kunna korta ner tiden mellan mätning och analys.
5. Gränssnitt för mikrovågsmätningar och avbildningarkan integreas ytterligare med maskininlärningsalgoritmer så att de klinkska mätningarna förbåttras så att det kan användas för att diagnostisera medicinska tillstånd.

Acknowledgment

First of all, I would like to express my gratitude to the Majlis Amanah Rakyat Malaysia for the scholarship during my studies, EUREKA Eurostars project COMFORT (E!9655), Swedish Vinnova project BDAS (2015-04159), H2020 Eureka Eurostars SenseBurn (E!12052), Swedish Vetenskaprådet (VR) project Osteodiagnosis (2017- 04644) and H2020 RIA – SINTEC (824984) consortium for the research funding. I would like to thank Anna Maria Lundin Foundation at Småland nation to provide me with travel grants to attend international conferences and courses.

During these 4 years, there are many people who have contributed to this thesis, directly and inderclty. I wish to express my deepest gratitude to:

My main supervisor, **Robin Augustine** for your utmost guidance and support to make this PhD thesis possible. Thank you so much for all the advice and discussion, for always being supportive, for the continuous dedication towards the accomplishment of the research work. It was a wonderful experience to be part of MMG team. And keep on baking amazing and delicious cake!

My co-supervisor, **Taco Blokhuis,** thank you for all your guidance concerning the medical advice and to show me the way to do things right for clinical perspective. It was bliss to share your expertise, answering all the questions I came up with and for being such pleasant persons to work with. My first to MMUC is still anchored in my mind. Thanks again for everything.

Anders For give me the opportunity to be part of a microwave group at Uppsala University. Thank you for all your support and encouragements.

Shi-Li Thank you for every fruitful discussion and advice that contribute the quality of this work and for every valuable feedback.

Jörgen For the assistance towards the accomplishment of the research work and in the preparation of the thesis.

Dhanesh, Thank you for your precious time to screen the thesis and give me valuable comments and suggestions for improvement.

Mauricio Your dedication to work was impressive. Thank you for the good advice, comment and many valuable discussions. Please take a small break when you can to keep your good health.

Roger Thank you for all the exciting exchange we have had, good tips and introduce me to Ironman race. I will prove I can survive for my first race and bit your best time! Ett enormt stort tack för Svensk sammanfattning.

Ida A. Thanks for being a great office-mate, for the amazing support and all great times during 4 years Ph.D. study in Uppsala, Sweden. Thank you for the friendship, the emotional support and the company during this thesis writing!

The one I considered brother, **Jacob**. That was an honour to be your closest friend! Thank you for being the best company, for the nice time travelling to the seminars and conferences. Let's continue supporting, encouraging and motivating each other. Let us keep the brotherhood alive!

Viktor For being such pleasant persons to work with. I hope you're happy to be in our office and wish you best of luck for your Ph.D. study. Thanks for the Svensk sammanfattning translation.

Microwave in medical engineering group members (past and present): **Sujith**, **Doo jin**, **John**, **George**, **Max**, **Joacim**, **Jasmin**, **Bappa**, **Pramod**, **Javad**, **Laya**, **Erik**, **Rocco**, **Jojo**, **Marwa**, **Abhishek**, and **Arvind**, for our scientific discussion during MMG meeting and fika, and for contributing to a great working atmosphere and gathering time.

Previous fellow colleagues in the Microwave group: **Dragos**, **Long**, **Imran** and **Renbin**. Thanks for fruitful collaboration and interesting discussion in the office.

My first officemate in the Ph. D student's office (past and present): **Patrik**, **Mandy**, **Olivier**, **Jie**, **Björn**, **Siddharth**, **Shuangshuang**, **XingXing**, **Chengyu**, and **Nishant.** Thanks for being great neighbours during my Ph.D. study and I have enjoyed every single moment in that office.

Ingrid, **Maria S.**, **Maria N.**, **Ramy** and **Ida N**. Thank you for taking care of the administration issue related to the studies.

Jonathan B For the IT support and help whenever I have technical problems with my PC.

My fika buddy, **Oleks**. Thanks for the good tips, chats and go-fikas times.

All my **colleagues in the FTE** (past and present), thank you so much for contributing toward a great and positive working environment, for all the presentation and valuable discussion during Friday fika meeting, for the parties and activities.

All my **COMFORT**, **BDAS, Senseburn**, **Osteodiagnosis** and **Sintec project members**. Thanks for the assistance and the various scientific and non-scientific discussion throughout the study.

My heartfelt appreciation is extended to: Malaysian friends in Sweden (past and present): **Maisarah, Fadli**, **Sahar**, **Syikin**, **Nasir**, **Ann**, **Adila, Izwan**, **Khadijah**, **Abg Mat, Yasmin**, **Salman**, **Muzaffar, Dalina**, **Akma**, **Malaysian in Stockholm**, **Malaysian Ambassador** to Sweden and **Embassy staffs**. I am grateful for the celebrations, food, gathering, fun and the feeling to be at home no matter where we are.

Duen and **Mona**, thank you introducing me to Robin during my first visit to Uppsala. Never give up hope, and never stop believing. Big dreams turn into big reality! To **Zoinol**, thanks for being a great mentor and advisor. I will always be grateful.

My SocMed colleagues especially: **Ada**, **Muz**, **Muney**, **Sharim**, **Peng**, **Khairil**, **Maoz**, **Wak Daoz**, **Shepa**, **Hashela**, **Burt**, **Abir**, **Ajid**, **Don**, **Jeju** (thank you for kad raya!), **Amirul, Hatta, Hajar** and **Yani**. Thank you for being good SocMed entertainer and supporter far from home during these past 4 years. To **Nana**, **Tirah**, **Aizat**, **Safwan**, **Alwi**, **Shah**, **Zura**, and **Dayah**, Thank you for your continued support. We will keep in touch!

I would like to dedicate my special appreciations to my family, without whom I probably could not be where I am today. Kepada **Mohd Shah**, **Ramlah Sudin**, **Suffiyan Radzi** dan keluarga, **Saidah Raihana** dan keluarga, **Syazwan Rahimi**, **Syahrul Firdaus** (Al-Fatihah), **Syahmira Farhana**, **Aisah Sudin** dan keluarga, **Jaafar Sudin** dan keluarga, terima kasih atas doa yang tidak pernah putus, cinta dan sokongan tanpa belah bagi. Along sayang kamu semua.

And lastly, to **all the people** who have given me their support, encouragement, advice, either directly or indirectly throughout my Ph.D. study in Uppsala, I say a thousand thank you. For that, I am forever grateful.

Uppsala, Sept 18th 2019.

References

1. Hollmann, H. E. Das problem der behandlung biologischer körper. *Ultrakurzwellen in ihren medizinischbiologischen Anwendungen*, Leipzig, **1938**, Chap. 4, 232.
2. Hemingway, A. and Stenstem, K. W. Physical characteristic of short wave diathermy. *Handbook of physic therapy, American Med. Assoc. Press*., Chicago, Ill., **1939**, 111(25), 2298–2302.
3. Lin, J. C., Kantor, G., and Ghods, A. A class of new microwave therapeutic applicators. *Radio Sci.*, **1982**, 17(5S), 119S–123S.
4. Michaelson, S. M., and Lin, J. C. Biological effects and health implications of radiofrequency radiation. *Springer,* New York: Plenum, **1987**, Chap. 3, 47.
5. Diederich, C. J. Thermal ablation and high temperature thermal therapy: overview of technology and clinical implementation. *Int. J. Hyperthermia*, **2005**, 21(8), 745–753.
6. Chichel, A., Skowronek, J., Kubaszewska, M., Kanikowski, M. Hyperthermia – description of a method and a review of clinical applications. *Rep Pract Oncol Radiother.*, **2007**, 12(5), 267–275.
7. Hancock, C. P., Burn, P., Duff, C. I., et al. A new Wave in electrosurgery: a review of existing and introduction to new radio-frequency and microwave therapeutic systems. *IEEE Microwave Magazine*, **2015**, 16(2), 14–30.
8. Metev, S. M., and Veiko, V. P. Laser assisted microtechnology. *Springer*, Berlin, Germany, 2nd edition, **1998**.
9. Bakhru, R. N., and Schweickert, W. D. Intensive care ultrasound: I. Physics, equipment, and image quality. *Ann Am Thorac Soc*., **2013**, 10(5), 540–548.
10. Vorlíček, J., Vrbova, B., Vrba, J., et al. Prospective applications of microwaves in medicine. *Advances in Cancer Therapy*, **2011**, 23, 507–532.
11. Roemer, R. B. Engineering aspects of hyperthermia therapy. *Annu Rev Biomed Eng.,* **1999**, 1, 347–376.
12. Bansal, R. Battling cancer: The latest on microwave hyperthermia. *IEEE Microwave Magazine*, **2005**, 6(3), 32–34.
13. Diederich, C. J. Thermal ablation and high-temperature thermal therapy: Overview of technology and clinical implementation. *Int. J. Hyperthermia*, **2005**, 21(8), 745–753.
14. Fhager, A., Trefná, H. D., Takook, P., Yu, Y., et al. Microwave technology in medical diagnostics and treatment. *2015 IEEE MTT-S 2015 International Microwave Workshop Series on RF and Wireless Technologies for Biomedical and Healthcare Applications (IMWS-BIO),* **2015**, 133–134.
15. Simon, C. J., Dupuy, D. E., and Mayo-Smith, W. W. Microwave ablation: Principles and applications. *Radiographics*, **2005**, 25, 69–83.
16. Li, X., Bond, E. J., Van Veen, B. D., and Hagness, S. D., An Overview of ultra wideband microwave imaging via space-time beamforming for early-stage breast-cancer detection. *IEEE Antennas and Propagation Magazine*, **2005**, 47(1), 19–34.

17. Fear, E. C., Li, X., Hagness, S. C., and Stuchly, M. A. Confocal microwave imaging for breast cancer detection: localization of tumors in three dimensions. *IEEE Trans. Biomed. Eng.*, **2002**, 49(8), 812–822.
18. Semenov, S. Y., and Corfield, D. R. Microwave tomography for brain imaging: feasibility assessment for stroke detection. *Int. J. Antennas Propag.*, **2008**, 254830-1–254830-8.
19. Obeid, D., Sadek, S., Zaharia, G., and El Zein, G. Multitunable microwave system for touchless heartbeat detection and heart rate variability extraction. *Microw. Opt. Tech. Lett.*, **2010**, 52, 192–198.
20. Persson, M., Fhager, A., Trefná, H. D., Yu, Y., et al. Microwave-Based stroke diagnosis making global prehospital thrombolytic treatment possible. *IEEE Trans. Biomed. Eng.*, **2014**, 61(11), 2806–2817.
21. Scapaticci, R., Bucci, O. M., Catapano, I., Crocco, L. Differential microwave imaging for brain stroke followup. *Int. J. Antennas Propag.*, **2014**, 312528.
22. Solberg, L.E., Aardal, Ø., Berger, T., Balasingham, I., et al. Experimental investigation into radar-based central blood pressure estimation. *IET Radar, Sonar Navigation*, **2015**, 9(2), 145–153.
23. Li, X., Pancera, E., Zwirello, L., Wu, H., et al. Ultra wideband radar for water detection in the human body. *Proc. German Microw. Conf.*, **2010,** 150–153.
24. Chandra, R., Balasingham, I., Zhou, H., and Narayanan, R. M. Medical microwave imaging and analysis. *Medical Image Analysis and Informatics: Computer-aided Diagnosis and Therapy*, **2017**, 451–466.
25. Nikolova, N. K. Microwave imaging for breast cancer. *IEEE Microwave Magazine*, **2011**, 12(7), 78–94.
26. Sill, J. M., and Fear, E. C. Tissue sensing adaptive radar for breast cancer detection—Experimental investigation of simple tumor models. *IEEE Trans. Microw. Theory Tech.*, **2005**, 53(11), 3312–3319.
27. Tong, K. F., Dufour, A., Ge, L., and Luk, K. M. Beamscanning probe antennas for deep brain stimulation. In *Proceedings of the 5th European Conference on Antennas and Propagation (EUCAP)*, Rom, **2011**, 3488–3490.
28. Qian, H., Loizou, P. C., and Dorman, M. F. Phone-assistive devices based on bluetooth technology for cochlear implant users. *IEEE Transactions on Neural Systems Rehabilitation Engineering*, **2003**, 11(3), 282–287.
29. Karacolak, T., Hood, A. Z., and Topsakal, E. Design of a dual- band implantable antenna and development of skin mimicking gels for continuous glucose monitoring. *IEEE Trans. Microw. Theory Tech.*, **2008**, 56(4), 1001–1008.
30. Gruber, R., Koch, H, Doll, B. A., Tegtmeier, F., et al. Fracture healing in the elderly patient. *Experimental Gerontology,* **2006**, 41(11), 1080–1093.
31. Chughtai, K. A., Nemer, O. P., Kessler, A. T., and Bhatt, A. Post-operative complications of craniotomy and craniectomy*,* *Emergency Radiology*, **2019**, 26(1), 99–107.
32. Duffield, S. J., Ellis, B. M., Goodson, N., Walker-Bone, K., et al. The contribution of musculoskeletal disorders in multimorbidity: Implications for practice and policy. *Best Practice & Research Clinical Rheumatology*, **2017,** 31(2), 129–144.
33. Prince, M. J., Wu, F., Guo, Y., Gutierrez Robledo, L., et al. The burden of disease in older people and implications for health policy and practice. *The Lancet*, **2015**, 385(9967), 549–562.
34. Hoy, D. G., Smith E., Cross M., Sanchez-Riera, L., et al. The global burden of musculoskeletal conditions for 2010: an overview of methods. *Annals of the Rheumatic Diseases,* **2014**, 73**,** 982–989.

35. Storheim, K., and Zwart, J. Musculoskeletal disorders and the global burden of disease study. *Annals of the Rheumatic Diseases* **2014**, 73**,** 949–950.
36. Woolf, A. D., Vos, T., and March, L. How to measure the impact of musculoskeletal conditions. *Best Practice & Research Clinical Rheumatology*, **2010**, 24(6), 723–732.
37. Parkinson, L., Waters, D. L., and Franck, L. Systematic review of the impact of osteoarthritis on health outcomes for comorbid disease in older people. *Osteoarthritis and Cartilage*, **2017**, 25(11), **2017**, 1751–1770.
38. Rikshöft. Annual report 2015. Available at https://rikshoft.se/wp content/uploads/2013/07/Årsrapport_2015.pdf. Accessed Sept. 4, **2019**.
39. Pettersson, J., Palmerius, K. L., Knutsson, H., Wahlstrom, O., et al. Simulation of patient specific cervical hip fracture surgery with a volume haptic interface. *IEEE Trans. Biomed. Eng.*, **2008**, 55(4), 1255–1265.
40. Schapira, D., and Schapira, C. Osteoporosis: The evolution of a scientific term. *Osteoporosis International,* **1992**, 2(4), 164–167.
41. Gullberg, B., Johnell, O., and Kanis J. A. World-wide projections for hip fracture. *Osteoporosis International,* **1997**, 7(5), 407–413.
42. Casanova, M., Schindeler, A., Little, D., Müller, R., and Schneider, P. Quantitative phenotyping of bone fracture repair: a review. *Bonekey Rep*. **2014**, 3(550), 1–8.
43. Cohen, M. M, and MacLean R. E. Epidemiology of craniosynostosis. *Craniosynostosis: diagnosis, evaluation, and management*, New York: Oxford University Press*,* **2000**, 112–118.
44. Pearson, A., Matava, C. T. Anaesthetic management for craniosynostosis repair in children. *BJA Education*, **2016**, 16(2), 410–416.
45. Diagnosis: Craniosynostosis. Avaliable at https://cranioutah.com/diagnoses/craniosynostosis. Access Sept. 4, **2019**.
46. Zatriqi, V., Arifi, H , Zatriqi, S., Duci, S., Rrecaj, S.h., and Martinaj, M. Facial burns - our experience. *Mater Sociomed*. **2013**, 25(1), 26–27.
47. Burn. World Health Organization. Available at http://www.who.int/news-room/fact-sheets/detail/burns. Accessed Aug. 5, **2019**.
48. Derganc, M. A uniform classification of the depth of burns. *Research in burns.* Stuttgart: H. Huber Publishers, **1972**, 11, 708–712.
49. Shakespeare, P. Burn wound healing and skin substitutes. *Burns*, **2001**, 27(5), 517–522.
50. Jaspers, M. E. H. Beyond the skin: new insights in burn care. *PhD Dissertation*, Vrije Universiteit Amsterdam, **2018**, 254.
51. Wound care manual and clinical guidelines for nurses. Available at https://www.ausmed.com/cpd/articles/wound-care. Accessed Aug. 5, **2019**.
52. Mohd Shah, S. R., Velander, J., Perez, M. D., Joseph, L., Mattsson, V., Asan, N. B., Huss, F., and Augustine, R. Improved sensor for non-invasive assessment of burn injury depth using microwave reflectometry. *13th European Conference on Antennas and Propagation (EuCAP), Krakow, Poland*, **2019**, pp. 1-5.
53. Wawrzyk, M., Sokal, J., Andrzejewska, and E., Przewratil, P. The role of ultrasound imaging of callus formation in the treatment of long bone fractures in children. *Pol J Radiol*., **2015**, 80, 473–478.
54. Grigoryan, M., Lynch, J. A., Fierlinger, A. L., et al. Quantitative and qualitative assessment of closed fracture healing using computed tomography and conventional radiography. *Academic Radiology*. **2003**, 10(11), 1267–1273.
55. Webb, J., Herling, G,. Gardner, T., Kenwright, J., Simpson, A. H. Manual assessment of fracture stiffness. *Injury*, **1996**, 27(5), 319–20.

56. Babatunde, O. M., Fragomen, A. T., and Rozbruch, S. R. Noninvasive quantitative assessment of bone healing after distraction osteogenesis. *HSS J.* **2010**, 6(1), 71–78.
57. White, M. S. Three-dimensional computed tomography in the assessment of fracture in the acetabulum. *Injury*, **1991**, 22(1), 13–9.
58. Pogliani, L., Zuccotti, G.V., Furlanetto, M. et al. Cranial ultrasound is a reliable first step imaging in children with suspected craniosynostosis. *Childs Nerv Syst.*, **2017**, 33, 1545–1552.
59. Khatib, M., Jabir, S., O'Connor, E. F, and Philp, B. A systematic review of the evolution of laser doppler techniques in burn depth assessment. *Plastic Surgery International*, **2014**, 1–13.
60. Thatcher, J. E., Squiers, J. J, Kanick, S. C., King, D. R., et al. Imaging techniques for clinical burn assessment with a focus on multispectral imaging. *Advances in wound care*, **2016**, 5(8), 360–378.
61. Jaspers, M. H. E., van Haasterecht, L., van Zuijlen, P. P. M., et al. A systematic review on the quality of measurement techniques for the assessment of burn wound depth or healing potential. *Burns*, **2018**, 45(2), 261–281.
62. Persson, M., Fhager, A., Trefná, H. D. Microwave based diagnostics and treatment. *7th European Conference on Antennas and Propagation, EuCAP*, **2013**, 3118–3119.
63. Raman, S., Augustine, R., and Rydberg, A. Geometrical and dimensional dependance of skull implants on oseointegration analysis using microwave probe. *IEEE Conf. Antenna Measurements Applications (CAMA)*, **2014**, 1–4.
64. Lee, D., Nowinski, D., and Augustine, R. A UWB sensor based on resistively-loaded dipole antenna for skull healing on cranial surgery phantom models. *Microw Opt Technol Lett.*, **2018**, 60, 897–905.
65. Mathur, P., Kurup, D. G., and Augustine, R. Design of open ended circular waveguide for non-invasive monitoring of cranial healing in pediatric craniosynostosis. *1st IEEE MTT-S International Microwave Bio Conference (IMBIOC)*, Gothenburg, **2017**, 1–4.
66. Raman, S., Augustine, R., and Rydberg, A. Noninvasive osseointegration analysis of skull implants with proximity coupled split ring resonator antenna. *IEEE Trans. on Antennas and Propag.*, **2014**, 62(11), 5431–5436.
67. Asan, N. B., Noreland, D., Hassan, E., Mohd Shah, S. R., et al. Intra-body microwave communication through adipose tissue. *Healthc Technol Lett.,* **2017**, 4(4), 115–121.
68. Perez, M. D., Thomas, G., Mohd Shah, S. R., Velander, J., et al. Preliminary study on microwave sensor for bone healing follow-up after cranial surgery in newborns. *12th European Conference on Antennas and Propagation (EuCAP),* **2018**, 1–5.
69. Velander, J., Mohd Shah, S. R., Perez, M. D., Asan, N. B., et al. A four-layer phantom for testing in-vitro microwave-based sensing approach in intra-cranial pressure monitoring," *IEEE MTT-S International Microwave Bio Conference (IMBIOC)*, Philadelphia, **2018**, 49–51.
70. Lee, D., Velander, J., Blokhuis, T. J., Kim, K., and Augustine, R. Preliminary study on monitoring the progression of osteoporosis using UWB radar technique in distal femur model. *Electronics Letters*, **2016**, 52(8), 589–590.
71. Polk, C., and Postow, E. Handbook of biological effects of electromagnetic fields. *CRC Press*, 2nd Edition, **1996**.
72. Hooker, G. A Practical guide to the determination of human exposure to radiofrequency fields. *Occup Environ Med*, **1995**, 52(7), 496.

73. Li, X. Body matched antennas for microwave medical applications. *PhD Dissertation*, KIT Scientific, **2014**, 230.
74. Feldman, Y., Puzenko, A., and Ryabov, Y., Dielectric relaxation phenomena in complex materials. *John Wiley & Sons, Inc*., **2005**, 1–125.
75. Gabriel, C., Gabriel, S., and Corthout, E. The dielectric properties of biological tissues: I. literature survey. *Phys. Med. Biol.*, **1996**, 41(11), 2231–2249.
76. Gabriel, S., Lau, R. W., and Gabriel, C. The dielectric properties of biological tissues: III. Parametric models for the dielectric spectrum of tissues. *Phys. Med. Biol.*, **1996**, 41(11), 2271–2293.
77. Markx, G. H., and Davey, C. L. The dielectric properties of biological cells at radiofrequencies: applications in biotechnology. *Enzyme and Microbial Technology*, **1999**, 25(3-5), 161–171.
78. Debye, P. Polar molecules. Dover Publications, New York, *J. Chem. Technol. Biotechnol.,* **1960**, 48, 1036–1037.
79. Melia, G. Electromagnetic absorption by the human body from 1–15 GHz. *Ph.D Thesis*, University of York, York, UK, August **2013**, 170.
80. Gabriel, S., Lau, R. W., and Gabriel, C. The dielectric properties of biological tissues: II. Measurements in the frequency range 10 Hz to 20 GHz. *Phys.Med. Biol.*, **1996**, 41(11), 2251–2269.
81. La Gioia, A., Porter, E., Merunka, I., Shahzad, A., Salahuddin, S., et al. Open-ended coaxial probe technique for dielectric measurement of biological tissues: challenges and common practices. *Diagnostics*, **2018**, 8(2), 40.
82. Peyman, A., Holden, S., and Gabriel, C. Mobile Telecommunications and Health Research Programme: Dielectric Properties of Tissues at Microwave Frequencies; *Microwave Consultants Limited*, London, UK, **2005**.
83. The "Nello Carrara" Institute of Applied Physics (IFAC). Dielectric properties of body tissues: in the frequency range 10 Hz–100 GHz. Available at http://niremf.ifac.cnr.it. Accessed Feb. 19, **2018**.
84. O'Rourke, A. P., Lazebnik, M., Bertram, J. M., Converse, M. C., et al. Dielectric properties of human normal, malignant and cirrhotic liver tissue: in vivo and ex vivo measurements from 0.5 to 20 GHz using a precision open-ended coaxial probe. *Phys. Med. Biol*., **2007**, 52, 4707–4719.
85. Lopresto, V., Pinto, R., Lovisolo, G., and Cavagnaro, M. Changes in the dielectric properties of ex vivo bovine liver during microwave thermal ablation at 2.45 GHz. *Phys. Med. Biol*. **2012**, 57, 2309–2327.
86. Keysight Technologies. Keysight 85071E Materials measurement software. *Keysight Technologies*, Santa Clara, CA, USA, **2015**.
87. Keysight Technologies (formerly Agilent Technologies). Basics of measuring the dielectric properties of materials. *Keysight Technologies*, Santa Clara, CA, USA, **2005**.
88. Chen, L. Ong, C. K., Neo, C. P., Varadan, V. V., and Varadan, V. K. Microwave electronics: measurement and materials characterization. *John Wiley & Sons*, UK, **2004**.
89. Gao, C., Wei, T., Duewer, F., Lu, Y., and Xiang, X. D. High spatial resolution quantitative microwave impedance microscopy by a scanning tip microwave near-field microscope. *Applied Physics Letters*, **1997**, 71(13), 1872–1874.
90. Xu, D. M., Liu, L., and Jiang, Z. Measurement of the dielectric properties of biological substances using an improved open-ended coaxial line resonator method. *IEEE Trans. Microw. Theory Tech*., **1987**, 35 (12), 1424–1428.
91. Gutmann, R. J., Borrego, J. M., Chakrabarti, P., et al. Microwave scanning microscopy for planar structure diagnostics. *IEEE MTT-S International Microwave Symposium Digest*, Palo Alto, CA, USA, **1987,** 281–284.

92. Abu-Teir, M., Golosovsky, M., and Davidov, D. Near-field scanning microwave probe based on a dielectric resonator. *Review of Scientific Instruments*, **2001**, 72(4), 2073–2079.
93. Ireland, D., and Abbosh, A. Modeling human head at microwave frequencies using optimized Debye models and FDTD method. *IEEE Trans Antennas Propag*. **2013**, 61(4), 2352–2355.
94. Mohd Shah, S. R., Velander, J., Mathur, P., Perez, M.D., Asan, N.B., et al. Split-ring resonator sensor penetration depth assessment using in vivo microwave reflectivity and ultrasound measurements for lower extremity trauma rehabilitation. *Sensors*, **2018**, 18, 636.
95. Mohd Shah, S. R., Mattsson, V., Velander, J., Perez, M.D., Vries, E.M., et al. Microwave-sensor-based clinical measurements for monitoring post-craniotomy bone development in pediatric craniosynostosis patients. *Sensors*, **2019**, Submitted.
96. Abbas, S. M., Desai, S. C., Esselle, K. P., Volakis, J. L. and Hashmi, R. M. Design and characterization of a flexible wideband antenna using polydimethylsiloxane composite substrate. *International Journal of Antennas and Propagation*, **2018**, 1–6.
97. Koulouridis, S., Kiziltas, G., Yijun, Z., Hansford, D. J., and Volakis, J. L. Polymer-ceramic composites for microwave applications: fabrication and performance assessment. *IEEE Trans. Microw. Theory Tech*., **2006**, 54(12), 4202–4208.
98. McDonald, J. C., and Whitesides, G. M. Poly(dimethylsiloxane) as a material for fabricating microfluidic devices. *Acc. Chem. Res.*, **2002**, 35(7), 491–499.
99. Mohd Shah, S. R., Velander, J., Perez, M. D., Joseph, L., Mattsson, V., et al. Improved sensor for non-invasive assessment of burn injury depth using microwave reflectometry, *13th European Conference on Antennas and Propagation (EuCAP),* Krakow, Poland, 2019, 1–5.
100. Keysight Technologies. N1501A Dielectric Probe Kit 10 MHz to 50 GHz: Technical Overview,. Available at http://www.keysight.com/en/pd-2492144-pn-N1501A/dielectric-probe-kit. Accessed Oct. 30, **2018**.
101. Keysight Technologies. N9918A FieldFox Handheld Microwave Analyzer, 26.5 GHz, Keysight Technologies, Inc., Application Note: 5990-9783EN, Santa Clara, CA, **2014**.
102. Velander, J. Microwave phantoms for craniotomy and bone defect monitoring. In *Dissertation*, Uppsala University, 23 June **2015**.
103. Mini Radio Solution. MiniVNA Tiny 1 MHz–3 GHz, Available at http://www.miniradiosolutions.com. Accessed Feb. 19, **2018**.
104. Mattsson, V. Clinical data analysis for conceptual proof of microwave bone healing monitoring system for craniosynostosis patients. In *Dissertation*, Uppsala University, 13 June **2018**.
105. Thomas, G. G. Extraction of follow up parameters of bone density microwave sensor from post craniotomy and lower extremity trauma rehabilitation measurements. In *Dissertation*, Uppsala University, 19 April **2018**.
106. Perez, M.D., Thomas G., Mohd Shah, S. R., Velander, J., et al. Preliminary study on microwave sensor for bone healing follow-up after cranial surgery in newborns. *12th IEEE European Conference on Antenna and Propagation (EuCAP)*, London, UK, 9–19 April **2018**, 1–5.

107. Perez, M. D., Mattsson, V., Mohd Shah, S. R., Velander, J., Asan, N. B., et al. New approach for clinical data analysis of microwave sensor based bone healing monitoring system in craniosynostosis treated pediatric patients. IEEE Conference on Antenna Measurements and Applications (CAMA), Västerås, Sweden, 3–6 Sept. **2018**, 1–4.
108. Vallauri, R., Bertin, G., Piovano, B., and Gianola, P. Electromagnetic field zones around an antenna for human exposure assessment: evaluation of the human exposure to EMFs. *IEEE Antennas Propag. Mag.,* **2015**, 57(5), 53–63.
109. King, R.W.P. Electric fields induced in cells in the bodies of amateur radio operators by their transmitting antennas. *IEEE Trans. Microw. Theory Tech*. **2000**, 48(11), 2155–2158.
110. King, R.W.P. Electric current and electric field induced in the human body when exposed to an incident electric field near the resonant frequency. *IEEE Trans. Microw. Theory Tech*., **2000**, 48(9), 1537–1543.
111. Asan, N.B., Noreland, D., Hassan, E., Mohd Shah, S. R., Rydberg A., et al. Intra-body microwave communication through adipose tissue. *Healthc Technol Lett.*, **2017**, 4(4), 115–121.
112. Asan, N.B., Penichet, C.P., Mohd Shah, S. R., Noreland, D., Hassan, E., et al. Data packet transmission through fat tissue for wireless intra-body networks. *IEEE J. Electromag. RF Microw. Med. Biol*., **2017**, 1(2), 43–51.
113. Raaben, M., Mohd Shah, S. R., Augustine, R., and Blokhuis T. J. COMplex Fracture Orthopedic Rehabilitation (COMFORT) - Real-time visual biofeedback on weight bearing versus standard training methods in the treatment of proximal femur fractures in the elderly: study protocol for a multicenter randomized controlled trial. *Trials.* **2018**, 19(1), 220.
114. Johnson, D., Wilkie, A. O. Craniosynostosis. *Eur J Hum Genet.* **2011**, 19(4), 369–376.
115. Perez, M. D., Jeong, S. H., Raman, S., Nowinski, D., Wu, Z., Mohd Shah, S. M., Velander, J., Peng, Z., Hjort, K., Augustine, R. Head-compliant microstrip split ring resonator for non-invasive healing monitoring after craniosynostosis-based surgery. *Healthcare Technology Letters*, Aug, **2019**, Accepted.
116. Mohd Shah, S. R., Asan, N. B., Velander, J., Ebrahimizadeh, J., Perez, M. D., Mattsson, V., Blokhuis, T., Augustine, R. Analysis of Thickness Variation in Biological Tissues using Microwave Sensors for Health Monitoring Applications. *IEEE Access*, **2019**, Submitted.

Appendices

Appendix A

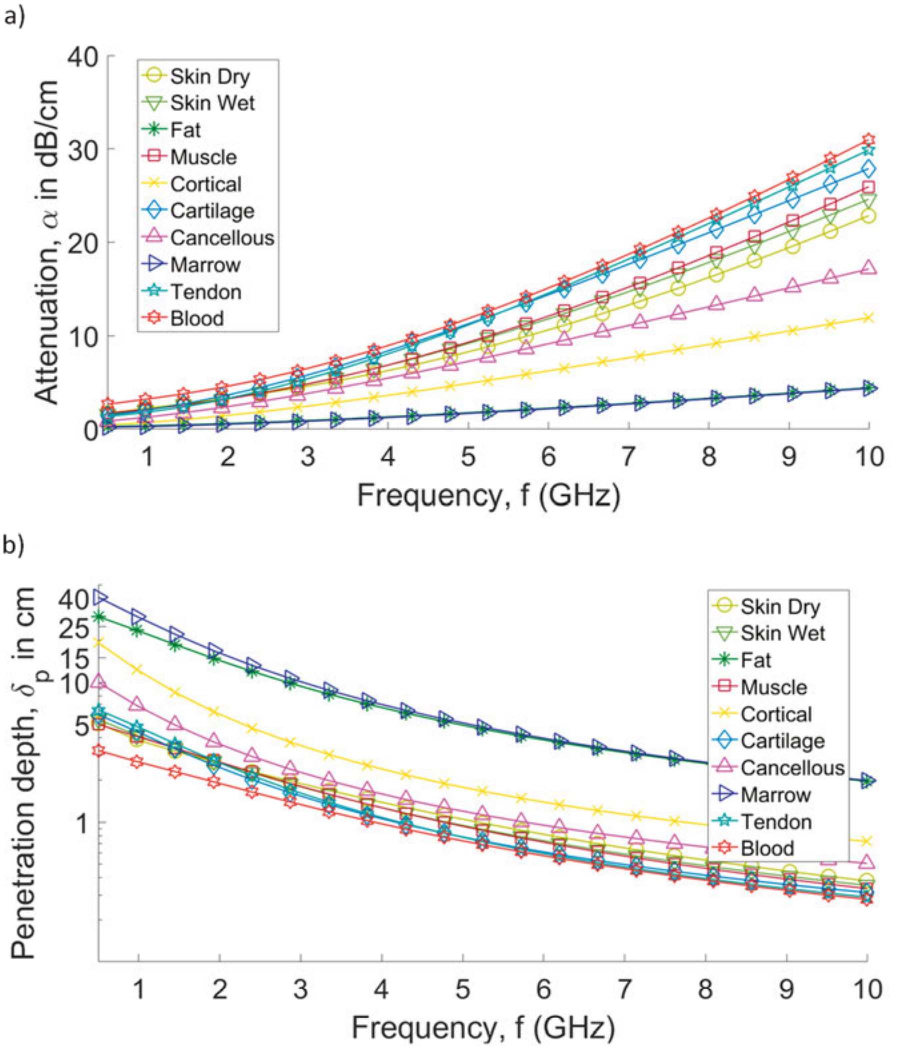

Figure A1. a) Attenuation b) Penetration depth of different human tissues over frequency for lower extremity trauma and burn injuries.[83]

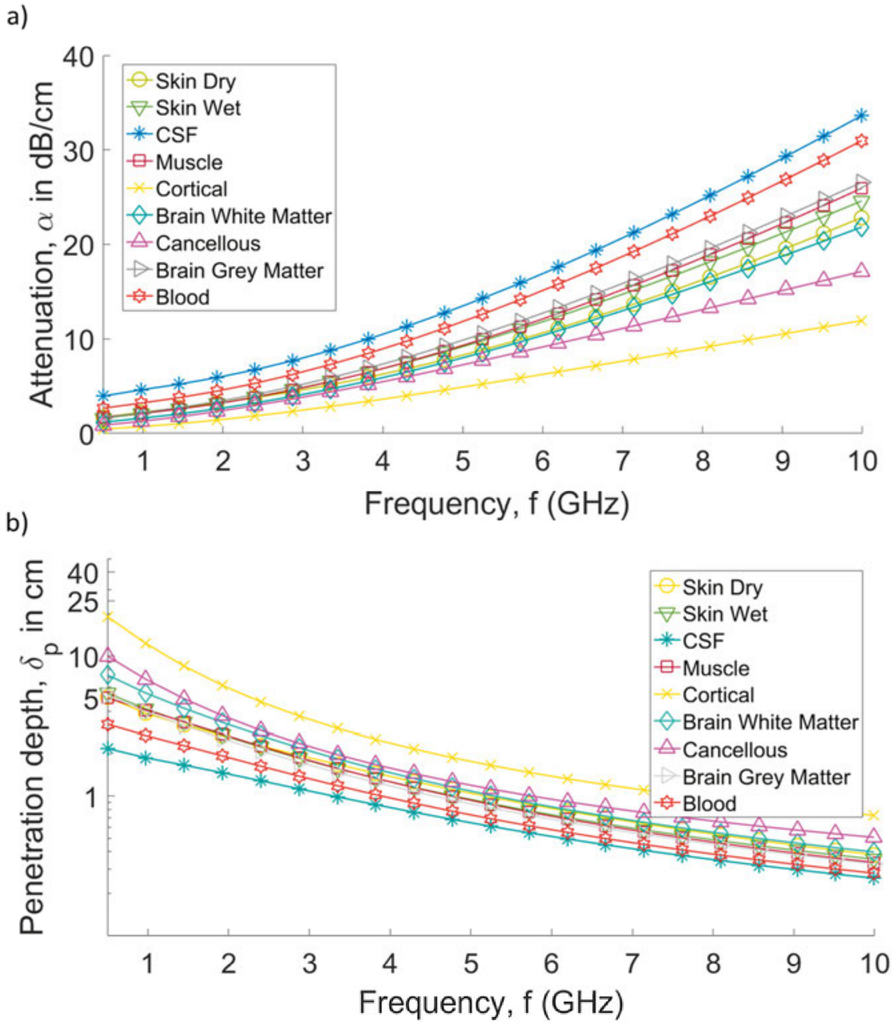

Figure A2. a) Attenuation b) Penetration depth of different human tissues over frequency for craniosynostosis.[83]

Appendix B

NOTIFICATION OF EXEMPTION

Research: "COMplex Fracture Orthopedic Rehabilitation (COMFORT) in elderly monitored by the SensiStep and Bone Density Analyzer", registered under number P1602.

Documents received:

Section		Document	Version Date
A	A1	Cover letter M. Raaben (email)	14 December 2015
C	C1	Research protocol	V1.0/14 December 2015
D	D6	Declaration of conformity SensiStep	11 December 2013
E	E1	Information letter for participants	Version 1/14 December 2015
	E2	Informed consent form	Version 1/14 December 2015

The accredited Ethics Committee (Dutch acronym: METC, English: MREC) Slotervaart Hospital and Reade reviewed above-mentioned study by expedited review and determined, based on the Dutch Medical Research Involving Human Subjects Act (Dutch acronym: WMO), that the research activities described meet the requirements for exemption from METC review under the WMO.

The protocol is in accordance with the Dutch Medical Treatment Act (Dutch acronym: WGBO) and the Dutch Data Protection Act (Dutch acronym: WBP).

Thank you for keeping the METC informed. Should any change occur to the study procedures, please contact the METC office regarding the statutory and policy requirements for METC review.

Statement of compliance
The METC Slotervaart Hospital and Reade is recognised by the Central Committee on Research involving Human Subjects (Dutch acronym: CCMO) and is authorised to carry out the ethical review of clinical trials.

Yours sincerely,
On behalf of the METC Slotervaart Hospital and Reade

C.H.W. Koks
Hospital pharmacist and clinical pharmacologist

Date: 15/01/2016

106088/SLZ 019

Reade
revalidatie | reumatologie

slotervaartziekenhuis

Appendix C

1

Dnr 2016 / 086

BESLUT
2016-03-23

SÖKANDE FORSKNINGSHUVUDMAN

Landstinget i Uppsala län
Box 602
751 25 UPPSALA

Forskare som genomför projektet:

Daniel Nowinski
VO Plastikkirurgi och käkkirurgi
Akademiska sjukhuset
751 85 UPPSALA

UPPGIFTER OM FORSKNINGSPROJEKTET ENLIGT ANSÖKAN INKOMMEN TILL NÄMNDEN 2016-02-29

Projektbeskrivning:

Mikrovågsteknik för analys av benbildning, bendefekter och benkvalitet hos patienter opererade för kraniosynostos.

Regionala etikprövningsnämnden i Uppsala meddelar följande

BESLUT

Nämnden bifaller ansökan och godkänner med stöd av 6 § lagen (2003:460) om etikprövning av forskning som avser människor den forskning som anges i ansökan.

Villkor

Forskningspersonsinformationen ska inledas med en tydlig *"Tillfrågan om deltagande i en forskningsstudie"*.

Adress	Telefon	Fax	E-post
Box 1964 751 49 Uppsala	018-4717400	018-4717410	registrator@uppsala.epn.se

REGIONALA ETIKPRÖVNINGSNÄMNDEN
EPN
UPPSALA

Dnr 2016 / 086

Erinran

Godkännandet upphör att gälla om forskningen inte har påbörjats inom två år efter slutgiltigt beslut.

BESLUTET FÅR ÖVERKLAGAS
Se anvisning.

På nämndens vägnar

Per-Erik Nistér
ordförande

Beslutande:
Per-Erik Nistér, f.d. rådman, ordförande
Ledamöter med vetenskaplig kompetens
Albert Alm, oftalmiatrik - föredragande, Brita Karlström, geriatrik, Lars von Knorring, psykiatri, vetenskaplig sekreterare, Carin Muhr, neurologi, Peter Nygren, onkologi, Susan Pfeifer, pediatrik, Bengt Simonsson, hematologi, vetenskaplig sekreterare, Agneta Yngve, nutrition
Ledamöter som företräder allmänna intressen
Helena Busch-Christensen, Görel Korkman, Margareta Åkerlind Skuteli

Expedieras till:
Forskare: Daniel Nowinski
Forskningshuvudmannens företrädare: verksamhetschef Gunilla Nygård

Adress	Telefon	Fax	E-post
Box 1964 751 49 Uppsala	018-4717400	018-4717410	registrator@uppsala.epn.se

EPN
REGIONALA ETIKPRÖVNINGSNÄMNDEN • UPPSALA •

Dnr 2016 / 086

Hur man överklagar etikprövningsnämndens beslut

Vem får överklaga?

Överklagandet ska göras av **forskningshuvudmannen/ behörig företrädare.** Behörig företrädare får lämna skriftlig fullmakt till forskare som genomför projektet.

Var ska beslutet överklagas?

Nämndens beslut kan överklagas hos Centrala etikprövningsnämnden, Stockholm. Överklagandet ska dock skickas eller lämnas till: Regionala etikprövningsnämnden i Uppsala, Box 1964, 751 49 UPPSALA.

Har överklagandet inkommit i rätt tid överlämnar nämnden överklagandet och handlingarna till Centrala etikprövningsnämnden.

När ska beslutet senast överklagas?

Överklagandet ska ha kommit in till nämnden **inom tre veckor** från den dag Ni fick del av beslutet.

Vad ska överklagandet innehålla?

Överklagandet ska vara skriftligt och det ska vara undertecknat.

I skrivelsen ska Ni ange

- Ert namn, adress, personnummer/organisationsnummer och telefonnummer,

- vilket beslut som Ni överklagar t.ex. genom att ange beslutsdatum och ärendets diarienummer,

- hur Ni anser att nämndens beslut ska ändras och varför det ska ändras.

- eventuell fullmakt som bilaga.

Adress	Telefon	Fax	E-post
Box 1964 751 49 Uppsala	018-4717400	018-4717410	registrator@uppsala.epn.se

AKADEMISKA
SJUKHUSET

Uppsala 2015-02-27

To whom it may concern

Reference: 'Microwave Probe Based System for Monitoring Osteogenesis in Cranial Vaults and Other Bony Defects' project initiated by Dr. Robin Augustine, Microwave Group, Uppsala University.

On behalf of our organization, The Craniofacial center at Uppsala University hospital, we would like to express our support to the **Microwave Probe Based System for Monitoring Osteogenesis in Cranial Vaults and Other Bony Defects** project.

We treat patients with various types of acquired and congenital craniofacial conditions that require reconstructive craniofacial surgery. We believe that we can learn more about the pathologies that we treat from the innovative system that is contemplated by the project, and we expect that significant gains will be made through the systematic and structured methodology that is pursued during the project. If the system that is developed in the project can be successfully demonstrated during the validation tests we believe that there are several potentially important clinical applications within our own field of craniofacial surgery, as well as for other conditions where bone healing and regeneration is crucial for successful treatment and rehabilitation.

We also like to confirm that we are prepared to participate in the trials that will be executed during the project.

Best regards,

Daniel Nowinski, MD, PhD
Associate professor
Chief, plastic surgery
Director, Craniofacial center
Uppsala university hospital
Daniel.nowinski@akademiska.se

Appendix D

EPN
REGIONALA ETIKPRÖVNINGSNÄMNDEN · UPPSALA ·

Dnr 2018 / 410

BESLUT
2018-12-12

SÖKANDE FORSKNINGSHUVUDMAN

Region Uppsala

Forskare som genomför projektet:

Fredrik Huss

UPPGIFTER OM FORSKNINGSPROJEKTET ENLIGT ANSÖKAN INKOMMEN TILL NÄMNDEN 2018-09-26 SAMT INKOMMEN KOMPLETTERING 2018-11-08

Projekttitel:

Senseburn.

Regionala etikprövningsnämnden i Uppsala meddelar följande

BESLUT

Nämnden bifaller ansökan och godkänner med stöd av 6 § lagen (2003:460) om etikprövning av forskning som avser människor den forskning som anges i ansökan.

Erinran

Godkännandet upphör att gälla om forskningen inte har påbörjats inom två år efter slutgiltigt beslut.

Adress	Telefon	Fax	E-post
Box 1964 751 49 Uppsala	018-4717400	018-4717410	registrator@uppsala.epn.se

EPN
REGIONALA ETIKPRÖVNINGSNÄMNDEN · UPPSALA ·

Dnr 2018 / 410

På nämndens vägnar

Per-Erik Nistér
ordförande

Beslutande:
Per-Erik Nistér, f.d. rådman, ordförande
Ledamöter med vetenskaplig kompetens:
Peter Appelros, geriatrik, Kristina Arnrup, odontologi, Martin Björck, kärlkirurgi, Lars-Gunnar Gunnarsson, neurologi - föredragande, Ulf Högberg, obstetrik och gynekologi, Martin Höglund, hematologi, vetenskaplig sekreterare, Tom Lundin, psykiatri, Anna Sarkadi, pediatrik
Ledamöter som företräder allmänna intressen:
Helena Busch-Christensen, Ingrid Fredriksson, Margaretha Åkerlind Skuteli

Expedieras till:
Forskare: Fredrik Huss
Forskningshuvudmannens företrädare: verksamhetschef Gunilla Nygård

Adress	Telefon	Fax	E-post
Box 1964 751 49 Uppsala	018-4717400	018-4717410	registrator@uppsala.epn.se

Acta Universitatis Upsaliensis

Digital Comprehensive Summaries of Uppsala Dissertations from the Faculty of Science and Technology 1855

Editor: The Dean of the Faculty of Science and Technology

A doctoral dissertation from the Faculty of Science and Technology, Uppsala University, is usually a summary of a number of papers. A few copies of the complete dissertation are kept at major Swedish research libraries, while the summary alone is distributed internationally through the series Digital Comprehensive Summaries of Uppsala Dissertations from the Faculty of Science and Technology. (Prior to January, 2005, the series was published under the title "Comprehensive Summaries of Uppsala Dissertations from the Faculty of Science and Technology".)

Distribution: publications.uu.se
urn:nbn:se:uu:diva-393105

ACTA
UNIVERSITATIS
UPSALIENSIS
UPPSALA
2019